KINETICS OF THE FORMATION OF NICKEL FERRITE

A Dissertation
submitted in partial fulfilment
of the requirements for the degree
of
MASTER OF ENGINEERING
in
METALLURGICAL ENGINEERING
[EXTRACTIVE METALLURGY]

BY

A.P. HARIT

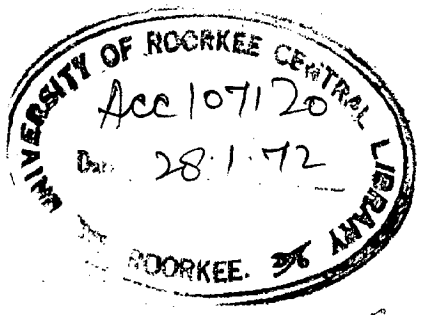

DEPARTMENT OF METALLURGICAL ENGINEERING
UNIVERSITY OF ROORKEE
ROORKEE
September 1971

CERTIFICATE

Certified that dissertation entitled "KINETICS OF THE FORMATION OF NICKEL FERRITE", which is being submitted by Sri A.P. Harit in partial fulfilment of the requirement for the award of Degree of Master of Engineering in EXTRACTIVE METALLURGY of University of Roorkee is a record of Student's own work carried out by him under my supervision and guidance. The matter embodied in this dissertation has not been submitted for the award of any other Degree or Diploma.

This is further to certify that he has worked for a period of about 8 months from Januaryl, 1971 to September 14, 1971 for preparing this dissertation.

S. K. Gupta

(S.K. Gupta)
Lecturer in Met. Engineering
University of Roorkee
ROORKEE, UP

Roorkee

Dated : Sept. 15, 1971

PREFACE

Previous kinetic studies on nickel ferrite formation by magnetic measurement methods were based on magnetic saturation measurement of fired samples. Blum and Li used a vibration specimen magnetometer which was similar to as described by foner . Similarly Economos and Clevenger applied a compensating coil magnetometer of the Weiss - forrer type to obtain the extent of reaction completed. The present work on the reaction kinetics of nickel forrite formation is based on the magnetic susceptibility measurement of the fired samples by Gony balance.

In the present investigation, an attempt has been made to study the effect of temperature on the reaction rate of nickel ferrite formation. The kinetics of this reaction is studied with elaboration on the rate equation which best fits the experimental data.

This thesis has been divided into four chapters. Chapter - I deals with the general introduction to the subject.

Literature review is included in Chapter - II. Besides the kinetics and mechanism of ferrite formation, some thermodynamic aspects of the solid - solid reaction are also discussed. It also includes a brief account of the methods of analysis and the factors effecting the kinetics of ferrite formation.

Chapter - III gives the description of the experimental set-up and procedure followed in the present investigation. Dense pellets of cylindrical shape of the stochiometric mixture of nickel oxide and ferric oxide were made by the mounting press, dried and then sintered at eight different temperatures. The kinetic data were obtained by measuring the weight increased by a semi-micro balance. The chemical analysis of fired samples were also done to confirm the results obtained by the magnetic susceptibility measurements.

Results obtained from the experiments carried out and a discussion on them constitute the subject matter of chapter IV. The experimental data are analysed by four reaction models - Jander, Ginestling - Brounshtlin, modified Ginstling - Brounstein and Kniger-Ziegler. The activation energies computed by the application of these models are 47.55, 46.26, 31.28 and 30.82 K cal/mole, respectivaly.

ACKNOWLEDGEMENTS

The author feels pleasure in expressing his sincere gratitude to Sri S.K.Gupta, Lecturer, Metallurgical Engineering Department, University of Roorkee, Roorkee, for his invaluable guidance, keen interest and constant encouragement at all times during the preparation of this thesis.

The author's special thanks are due to Dr.M.N.Saxena, Professor and Head of the Metallurgical Engineering Department for providing all the facilities to carry out this investigation.

Thanks are also due to Dr.W.U.Mallick, Professor and Head of the Chemistry Department, University of Roorkee, Roorkee, for allowing me to work on magnetic balance for susceptibility measurements in the Chemistry Department.

Author also wishes to express his thanks to Structural Engineering Research Centre, Roorkee for providing the computer facilities for setting various problems concerning this work on the computer.

The author also thanks the staff of Metallurgical Engineering Department for their help and cooperation.

Ahuja

A.P. Ahuja

Roorkee,
September 15, 1971

CONTENTS

LIST OF TABLES

LIST OF FIGURES

FIG.NO.

****

CHAPTER - I

****

The growing importance of ceramic magnets in the modern electronics industry led to the extensive researches and rapid growth of ferrite manufacturing industries. Although the first usable ferrite was made in 1946, now most of the magnetic components previously made of metallic magnets are being replaced by non - metallic ceramic magnets i.e. ferrites. Now a days, soft as well as hard ferrites are available with the required magnetic properties i.e. saturation magnetization and coercive force. Ferrites have very high resistivity (10^{7} ohm - metre as compared to 10^{-7} ohm - metre for iron) which gives very low eddy current losses even at microwave frequencies. Some of the important applications of ferrites are in fly back transformer, deflection yokes, magnetic memories, resonance insulator, television picture tube, IF transformers etc. The two recent developments in this field are (i) the production of thin ferrite films of the order of 1000 Å thickness by vacuum evaporation of the metals and subsequent high temperature oxidation, and (ii) the production of ultra-fine ferrite particles by chemical precipitation method.

Indeed, the work on the solid - solid type of reaction in ferrite formation is very old. Hilpert[1] in 1909 recognized the importance of these magnetic materials and examined some of them. The work of Rodvell[2], Tammann[3],

Jandor[4], and others in the early part of this century contributed immensely, both directly and indirectly, to the understanding of the reactions in ferrites. Cobb[5] in the United States, Kato and Takei[6] in Japan, and Forestier and Vetter[7] in France were among those who advanced ferrite technology greatly in the thirties. Before and during World War II, the Philips Company in Holland further developed these materials and described their properties extensively. Today, considerable effort is being put into the research and development of ferrites and related ceramic materials for use in the electronics industry.

Ferrites are ceramic ferromagnetic materials with the general chemical composition $MO.Fe_2O_3$, where M is a divalent metal such as iron, magnesium, nickel, zinc, cadmium, cobalt, copper, aluminum, manganese etc. or a mixture of these. The ferrites crystallise into the spinel structure. In contrast with the original premise that all ferro-magnetic ferrites are inverse, recent studies show that, although most ferrites tend towards the inverse configuration, they may exist with major deviation from this distribution.

The whole family of ferrite, according to Economos[8] may be divided into five basic groups. First group consists of normal spinel e.g. zinc ferrite : $(Zn)\left[Fe_2\right]O_4$

This ferrite is, nevertheless important in both the theoretical and practical understanding and utilization of ferrite. The second group ferrites have inverse structure e.g. nickel ferrite : $(Fe^{3+})\ [Ni^{2+}\ Fe^{3+}]\ O_4$ which is a stable ferromagnetic material too. Third group consists of ferrites whose cation arrangement may be altered by heat treatment and is exemplified by magnesium ferrite : $(Mg^{2+}_{1-x}\ Fe^{3+}_{x})\ [Fe^{3+}_{2-x}\ Mg^{2+}_{x}]\ O_4$. Fourth group reaction has a special case where only one starting component is used to form magnetite :

$$6Fe_2O_3 = 4Fe_3O_4 + O_2 \qquad \ldots \quad (1)$$

This is also an inverse ferrite : $(Fe^{3+})\ [Fe^{2+}\ Fe^{3+}]O_4$. Last group consists of ferrites which are formed by a combination of reaction of other group ferrites e.g. manganese ferrite.

The kinetics of the formation of nickel ferrite from its oxide components has been intensively studied by several workers. Kodendy and Katz[9] examined nickel ferrite and found that spinel formation occurs at about 700°C, and the reaction reaches its completion at about 1200°C. Economos and Clevenger[10] studied the effect of iron oxide particle size on the rate of nickel ferrite formation. Blum and Li[11] studied the effect of milling techniques, and particle shape and size of α - Fe_2O_3 on reaction kinetics of nickel ferrite.

Previous kinetic studies on nickel ferrite and other ferrite system have been interpreted in terms of a model of the reaction developed by Jander[4]. Later work found empirical expression derived by Tammann[3] more reliable. However, Blum and Li[11] developed a rate equation and verified it with their data and the data of Economos and Clevenger[10] on nickel ferrite and from the data of Frosh[12] on magnesium ferrite.

Out of the several mechanisms proposed, Wagner[13] mechanism of counter diffusion of cations through a relatively rigid oxygen lattice has gained considerable favour over the years. Other proposals involving the movement of oxygen ion and only one cation has not been experimentally verified.

Different experimental techniques have been adopted by various workers to study the reaction kinetics of ferrite. Economos[14], Okamira[15], Simoizeke and Jefferson[16] used saturation magnetization measurements. Kedesdy and Katz[9] employed x - ray method to follow the formation of ferrite structure. The microstructure and kinetics of magnesium ferrite were studied by Moore[17] by sandwich type diffusion couple method. Chufarov and Shchepotkin[18] employed x - ray quantitative phase analysis and specific magnetic saturation moment method to defect the degree of ferritization and the role played by surface and volume diffusion of magnesium and cobalt ferrite.

****

CHAPTER II

****

LITERATURE REVIEW

II.1 INTRODUCTION

Ferrite forming reactions fall in the group of addition type solid state reactions e.g.,

$$A\ (solid) + B\ (solid) = C\ (solid) \quad \ldots (2)$$

Because the reactant molecules cannot move freely in the solid state in sharp contrast to the reactions in other phases, usually they are diffusion controlled. Broadly speaking, there are two ways of studying the reaction kinetics of ferrite formation. One method is the use of intimately mixed powdered mixture of reacting oxides, which is also a most commonly used technique. Fresh and Dolling[19] studied the kinetics of MgO - Fe_2O_3 system from powder mixtures and concluded that the rate controlling step is the diffusion of oxide components through the ferrite layer. The other method is based on the use of a sandwich type diffusion couple. Moore[17] in his work on magnesium ferrite by the diffusion couple method found that the spinel growth follows a parabolic rate law, and the activation energy for the rate controlling step was 75 K cal/mole in the temperature range 1155° to 1340°C.

II.2 THERMODYNAMIC ASPECT OF FERRITE REACTIONS

In the solid - solid reactions, the thermodynamic activities of the reactant and the product

remain constant throughout the course of reaction, provided no appreciable changes in solid solubility occur. In general, the free energy change ΔG would be constant in the course of time, provided the temperature and pressure are kept constant, since the chemical potential and the activity of a pure solid are constant at constant temperature and pressure. Theoretically speaking when $\Delta G < 0$, the reaction should proceed to completion. Even where the reaction is favoured thermodynamically, it may not be favoured kinetically, since the solid state reactions are complicated by the fact that a layer of the reaction product builds up gradually at the interface and at least one of the reactants has to diffuse through this layer, if the reaction is to continue.

Now, ΔG is given by

$$\Delta G = \Delta H - T\Delta S \qquad \ldots \quad (3)$$

where ΔH and ΔS are the enthalpy and entropy changes during the reaction. Most of the evidence suggests that in many solid - state reactions, predominantly lattice arrangement is involved. In such cases, the degree of randomness is affected only to a small extent and hence:

$$\Delta S = 0$$

consequently, for a reaction to occur, $\Delta H < 0$. One would expect, therefore, that, in general, solid state

reactions should be exothermic. Novrotsky[20] and Kleppa[21] estimated the lattice entropies of formation of spinels from low temperature heat capacity measurements, for a few ferrites given in Table 1, which shows that these are really small.

The experimental measurements of enthalpy indicate that the enthalpies are small and usually negative. The enthalpy changes for a number of spinel formation reactions have been recently measured by Novrotsky[20] and Kleppa[21]. Some typical values are given in Table 2.

Very little information on change in volume in solid - state reactions is available. However, it appears that the volume changes in solid - state reactions are usually small.

In solid - state reactions, polymorphic changes are also possible, which are governed by the free energy of the phases. At any given temperature and pressure, the phases with the lowest free energy is most stable and the compound, therefore, tends to exist in this phase. If the temperature and pressure are changed, the condition of minimum free energy may require the compound to undergo transition from one phase to other.

The entropy of activation is an important parameter in solid - state reactions. The sign and magnitude of ΔS^{o}, the difference of the entropy of the reactant and the activated state during diffusion can give valuable indication about the diffusion mechanism. Duncan and Stewart[22] have evaluated ΔS^{o} for the reaction between ZnO and Fe_2O_3 for a wide temperature range. They conclude that since the enthalpy contribution to the free energy of activation is much smaller than the enthalpy term, the rate determining step would be associated with the transport of metal ions through the lattice.

II.3 EXPERIMENTAL METHODS TO STUDY THE KINETICS OF FERRITE FORMING REACTIONS

Ferrite forming reactions, being a solid - state reaction are very slow. The analysis of the reaction product is difficult and the estimation of the reactant concentration as a function of time is still more difficult. Consequently the study of reaction kinetics is more troublesome as compared to that in the gaseous and liquid phases. However, the solid - state reactions have to be studied below the eutectic temperatures of the mixture in order to avoid the appearance of the liquid phase. Several methods have been adopted to study the ferrite forming reactions

The following methods are commonly used to follow the course of ferrite reactions[23].

II.3.1 DIRECT ANALYSIS OF THE REACTION PRODUCTS

The direct analysis of the reaction products may be accomplished either by chemical analysis or by measuring the intensity of x - ray spectral lines. The chemical analysis methods are less accurate and it is also rarely possible to employ them. Hence, recort to the x - ray technique is usually made. X - ray technique suffers from many disadvantages. The intensity of the spectral lines depends on the crystallinity of the substance used. Thus, the presence of poorly crystalline intermediates in the mixture would hinder the detection of other phases owing to unduly heavy scattering by the specimen. Moreover, small amounts of the products can be detected with difficulty. The greatest disadvantage of this technique is that the composition determination by this method takes a very long time.

Guilliasen and van Rysselberghe[24] used the direct analysis method to study the kinetics of zinc ferrite. The unreacted zinc oxide was extracted with an ammonical solution of ammonium chloride. Kedesdy and Tauber[25] utilized x - ray diffraction, gravimetric, optical and magnetic measurement techniques to follow

the course of the manganese ferrite reaction. Chuferov and Shchepotkin[16] employed x - ray method to study the mechanism and kinetics of cobalt and magnesium ferrites.

II.3.2 THE MEASUREMENT OF PRODUCT LAYER THICKNESS

When a coloured product is formed, the thickness of the product layer may be determined at various time intervals. The measured thickness can be correlated with the kinetics of spinel formation. Moore[17] studied the kinetics and structure of magnesium ferrite by this method through a diffusion couple arrangement. The fired samples were prepared by the usual metallographic techniques and observed under an optical microscope with a micrometer mount substage. The product thickness were measured with an accuracy of 0.001 mm.

II.3.3 USE OF RADIO ACTIVE TRACERS

In some cases where the product formed is colourless, radioactive tracers may be used to assess the extent of movement of the reacting zone. The radioactive tracer technique used in the study of $MgCr_2O_4$ spinel, showed that the chromium penitration into single crystal of magnesium oxide takes place upto a distance of 300 microns after annealing for 17 hours at 1100°C.

II.3.4 ELECTRICAL CONDUCTIVITY MEASUREMENTS

The electrical conductivity is a good tool, provided the conductivity of the ferrite produced is

much different from the conductivity of its reactent oxides.

II.3.5 MAGNETIC MEASUREMENTS

Magnetic measurements are most commonly applied for the study of ferrite forming reactions, because the reaction product is generally a magnetic substance. Magnetic susceptibility measurements have been used to study the nickel ferrite formation, since the product has a higher magnetic susce-ptibility than the reactants. However, Blum and Li[11] used a vibrating specimen magnetometer for measuring the saturation magnetization of spheres of nickel ferrite. Economos and Clevenger[10] used a compensating coil magnetometer of the Weiss - Forrer type for magnetic moment measurement of nickel ferrite samples to compute the reaction rate.

II. 4 MECHANISM OF FERRITE FORMATION

In recent years the mechanism of solid - solid reactions has been examined by Lindner and Co-workers[26]. These investigators have usually compared the kinetics of ferrite formation with cation diffusion rates through the product layer and in few cases have made marker studies. Several mechanisms have been proposed for the ferrite formation from its constituent binary oxides. Of the several mechanism only Wagner's[13] mechanism of counter - current diffusion of cations within a rigid

oxygen network seems to fit the experimental observations in many cases. Other proposals which have also gained some importance considers the possibility of anion diffusion also. The comparision of the reaction and diffusion rates indicate that $ZnFe_2O_4$, $MgFe_2O_4$, $NiFe_2O_4$ etc. are formed by Wagner mechanism, although diffusion of O^{2-} ions is not excluded if the diffusion rate of O^{2-} ions were fortunately near that of cations. Earlier Hopkins[27] had indicated that Fe_2O_3 diffused through $ZnFe_2O_4$, although the evidence was only circumstantial.

Solid state reactions have certain specificity rega-rding their direction of propagation. In case of ferrite there are two possibilities, the product layer may advance towards one of the reactants or towards both. The later is more commonly observed. Considering the reaction between nickel oxide (A) and ferric oxide (B) to form nickel ferrite (AB) which is not miscible with either of the reactants. If A is capable of diffusing through AB while B is not, A will enter the product layer at the interface A/AB and combine with B at the interface AB/B, consequently, the product layer would move towards B and the situation will correspond to as shown in Fig. 1(i). However, if both the reactants A and B can diffuse through the product layer, the

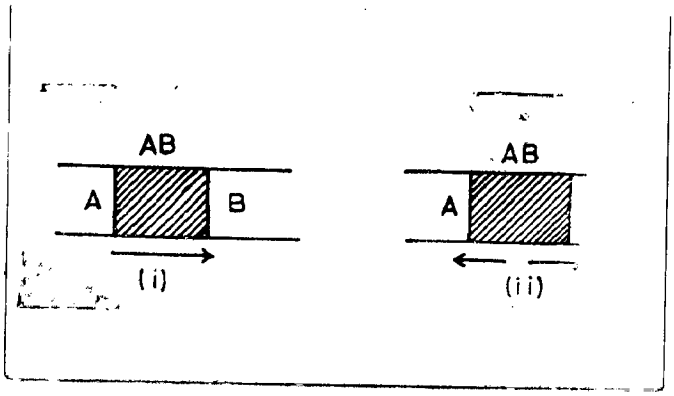

Fig. 1. Schematic representation of product layer movement; (i) when product layer moves towards one of the reactant (ii) when product layer moves towards both of the reactants.

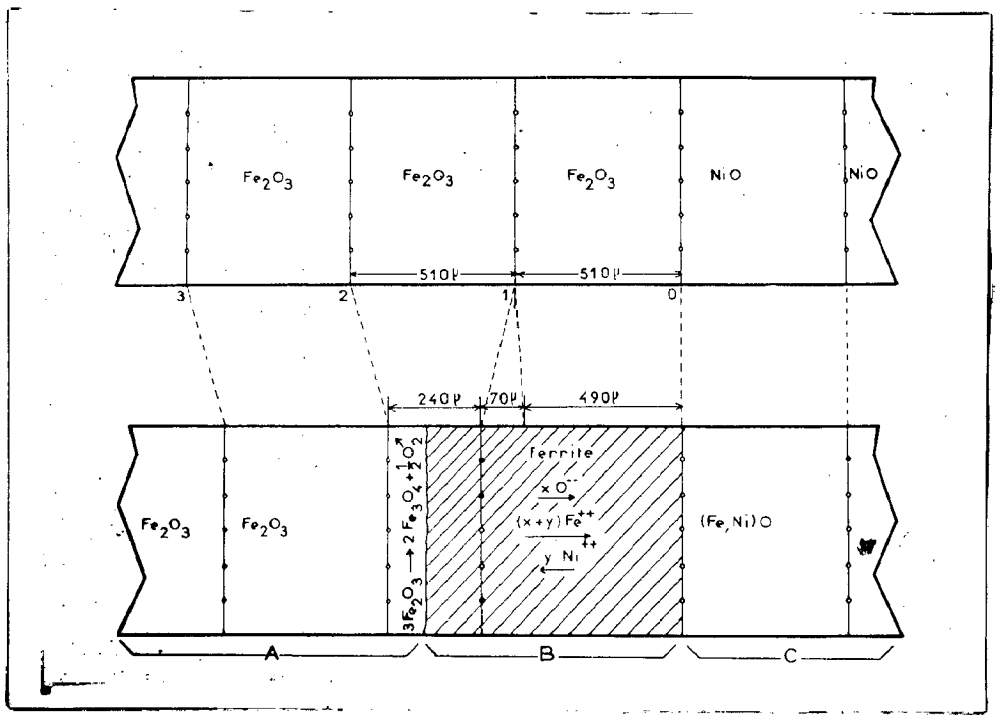

Fig. 2. Schematic representation of Fe_2O_3 and NiO diffusion in nickel ferrite formation for sample fired at 1315°C for 67 hr. in air[28].

boundary will move on both the sides as shown in Fig. 1(ii). A schematic representation of Fe_2O_3 and NiO diffusion, and microstructure, as observed by Paulus and Evans[28], is shown in Fig. 2 and 3, respectively, for a sample fired at 1315°C in air for 67 hours.

Generally, the factors determining the direction of propagation of reaction product are not fully known. However, where the vapour phase is involved, one may expect that the component having higher vapour pressure would probably have a greater tendency to diffuse in the product layer. In cases where the diffusion of different ions can occur (as in case of ferrite) across the reaction product, a considerable simplification can be achieved. Because in the steady state no space charge is created, SO, there is no net flow of electrical charge associated with mass flow. Considering the magnesium ferrite reaction as an example, out of many there are following two possible situations :

(a) If Mg^{2+} ions diffuse from one side and Fe^{3+} ions from the other, the respective number of ions simultaneously diffusing to maintain electroneutrality must be 3 and 2 (Fig.4). The product boundary will move along the both directions if diffusion proceeds in this manner. It is also obvious that the volume ratio

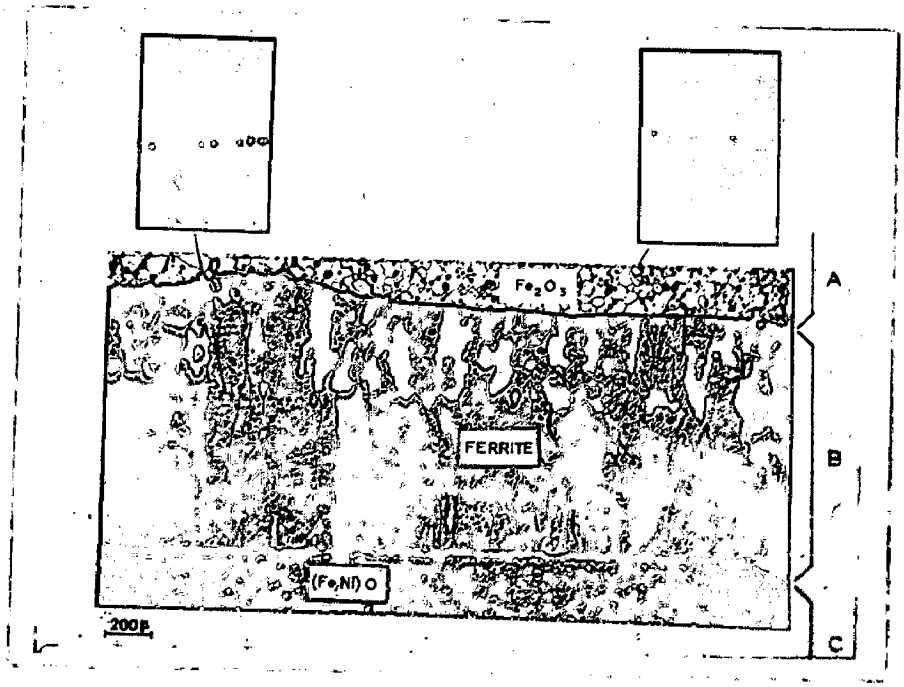

Fig. 3. A micrograph of sample ($NiFe_2O_4$) fired at 1315°C for 67 hour in air.[28]

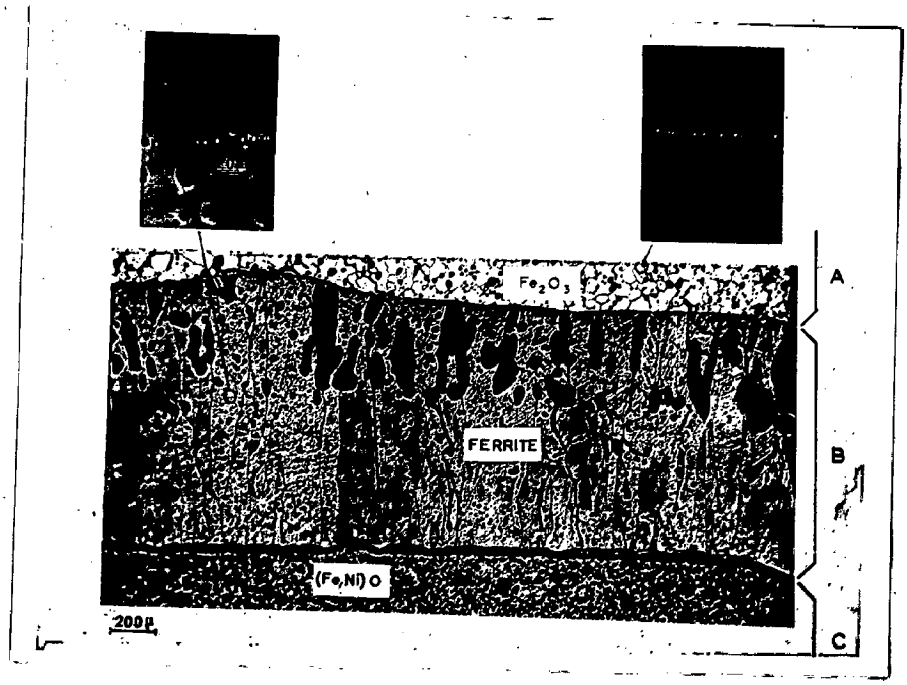

Fig. 3. A micrograph of sample ($NiFe_2O_4$) fired at 1315°C for 67 hour in air.[28]

of the product on the two sides of the initial line of separation would be 1:3. This situation was observed by Moore[17] in his diffusion couple type kinetic study of magnesium ferrite, and it is in accordance with the Wagner's[13] mechanism.

(b) If Fe^{3+} and O^{2-} alone diffuse, the state of affairs would be as shown in Fig. 5, to maintain the electro-neutrality. In this case the product boundary would move only in one direction, i.e. towards MgO.

For ascertaining the direction of diffusion two methods[29,30] have been applied in the case of ferrites. One is called the marker method, since in this procedure a mark is put at the initial surface and its subsequent position in the spinel layer is determined after the reaction has gone to a sufficient extent. In the second method, the texture of the product layer is analysed. Similar texture of the prodcut layer throughout gives indication of one sided diffusion. On the other hand, if the texture on the two sides of the initial surface can be distinguished, two - way diffusion is possible. However, it is frequently difficult to distinguish the texture on two sides. In the case of $MgO.Fe_2O_3$ system both the methods show that counter diffusion of ions occur through the product ferrite layer. The ratio of the two layers of different structure was found to be approximately 1:3. The results are

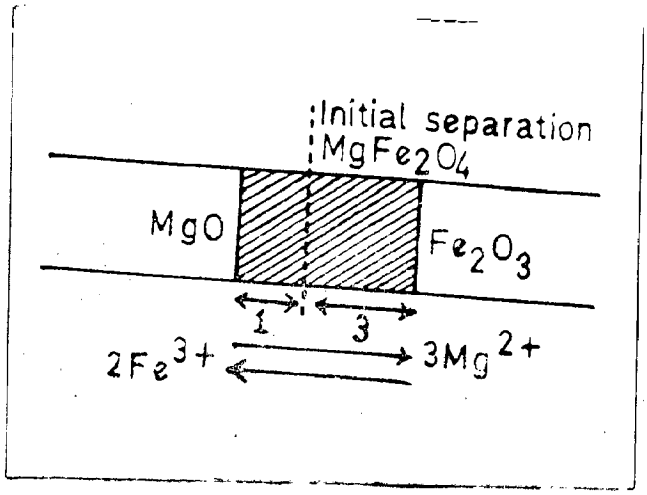

Fig. 4 - Schematic representation of diffusion; when diffusion of both the cations occur through the ferrite product layer.

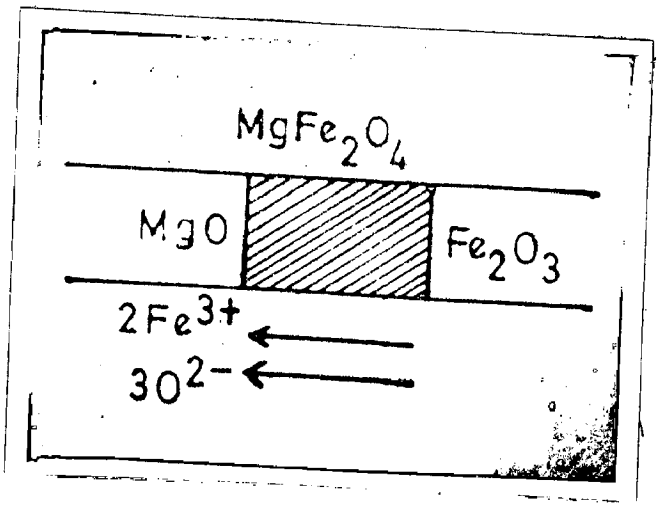

Fig.5 - Schematic representation of diffusion; when diffusion of only one cation with oxygen anion occur through ferrite product layer.

complicated by the fact that the system forms a MgO-Fe_2O_3 solid - solution, specially at high temperatures. The above considerations are useful when the gas phase transport through the crevices or pores, grain boundary diffusion or surface migration occurs. The situation has novel features when bulk diffusion is involved. Yamaguchi and Tokuda[31] investigated a series of spinel reactions and found evidence of one - sided diffusion in individual grains as shown in Fig. 6.

The mechanism of ferrite formation has been studied by Finch and Sinha[32] and by Nicholls[33] and they indicated that the formation of γ-Fe_2O_3 is a necessary precursor in the spinelization reaction. Their conclusions, however, are not completely supported by other work[30,35,36] on the stability of γ-Fe_2O_3 at high temperatures.

II.5 KINETICS OF FERRITE FORMATION

The course of a solid - solid reaction may be represented schematically in the following manner :

(1) In the proliminary stages reaction takes place at the interfaces of reactants. This state of affairs is shown in Fig. 7. A and B are the respective metallic ions present in the reacting oxides.

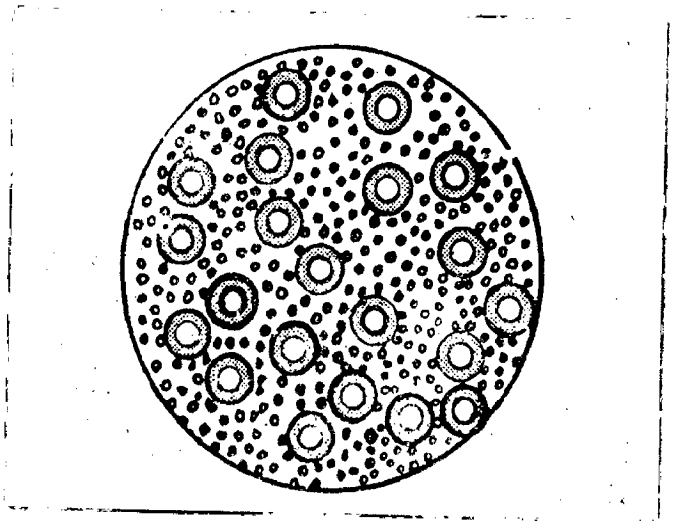

Fig. 6 - One - sided diffusion in individual grains of ferrite[31].

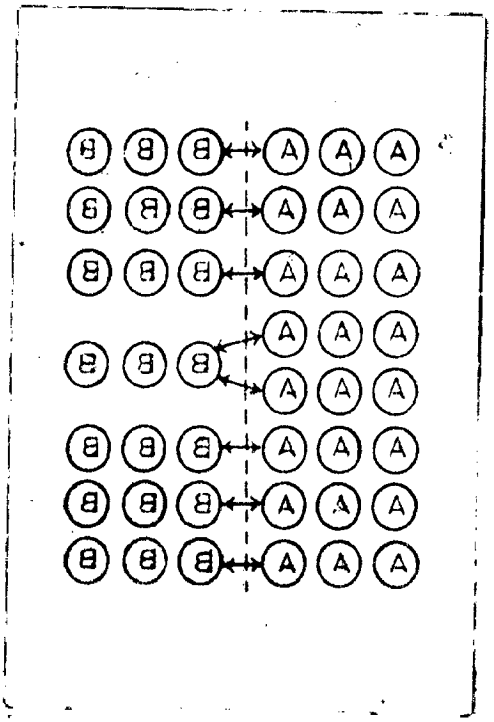

Fig. 7 - Preliminary stage - showing reaction at the interface of reactants.

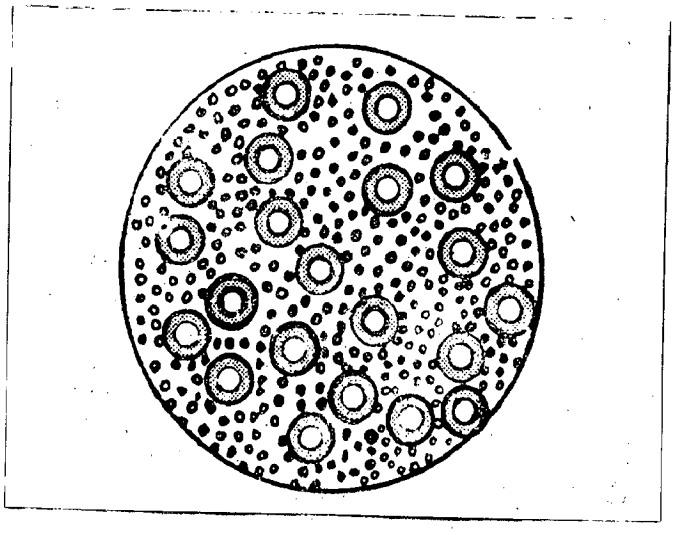

Fig. 6 - One - sided diffusion in individual grains of ferrite[31].

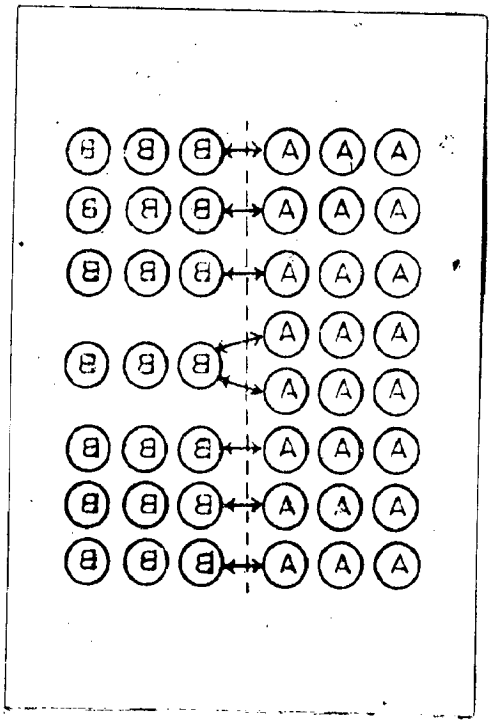

Fig. 7 - Preliminary stage - showing reaction at the interface of reactants.

(ii) Subsequently, the diffusion of a particular specie, 'A' occurs across the product layer either by vapour phase, surface or grain boundary diffusion. This is shown in Fig. 8.

(iii) Finally, propagation of the reaction in the individual grain of reactant 'B' would occur, as shown in Fig. 9.

Thus, in the overall kinetics of solid - state reactions, the following aspects are important :

(a) lateral diffusion of the reactants;

(b) bulk diffusion of the reactants in the grain;

and (c) nature and mechanism of the chemical reaction.

Several empirical rate laws have been proposed which describe the course of typical solid - state reactions. Reaction data were analysed using equations corresponding to four reaction mechanisms. The mechanisms and their specific rate equations are given below

II.5.1 <u>PRODUCT GROWTH CONTROLLED BY DIFFUSION OF REACTION THROUGH A CONTINUOUS PRODUCT LAYER</u>

In models of this type three assumptions are made (a) the reactant particles are spheres (b) surface diffusion rapidly covers reactant particles with a continuous product layer during the initial stages of

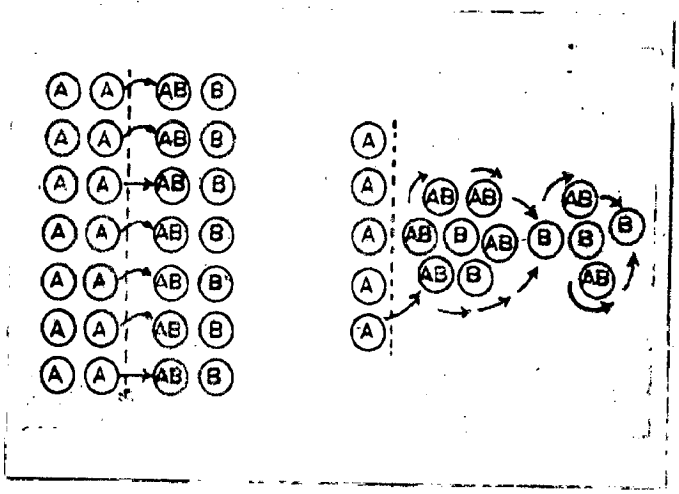

Fig. 8 - Diffusion of one reactant through the product layer.

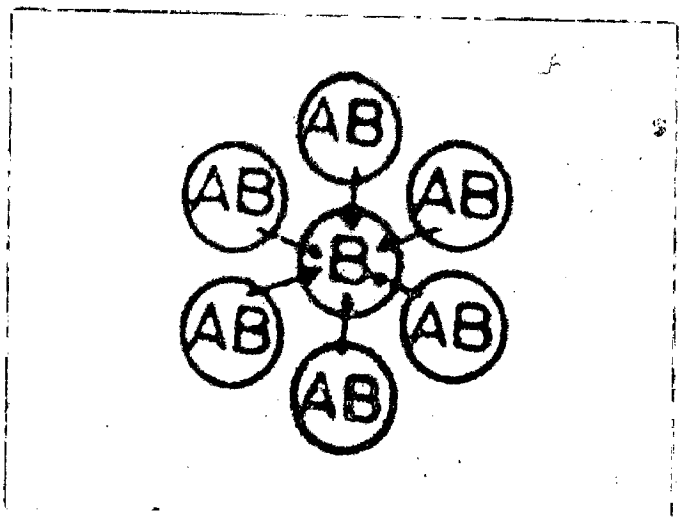

Fig. 9. - Propagation of the reaction in the individual grains.

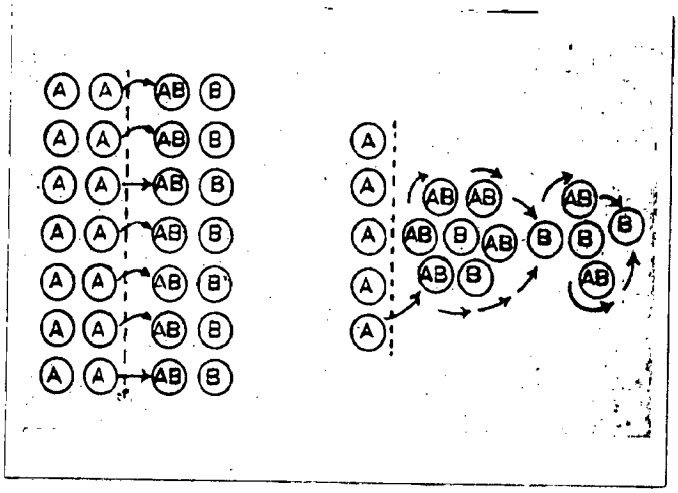

Fig. 8 - Diffusion of one reactant through the product layer.

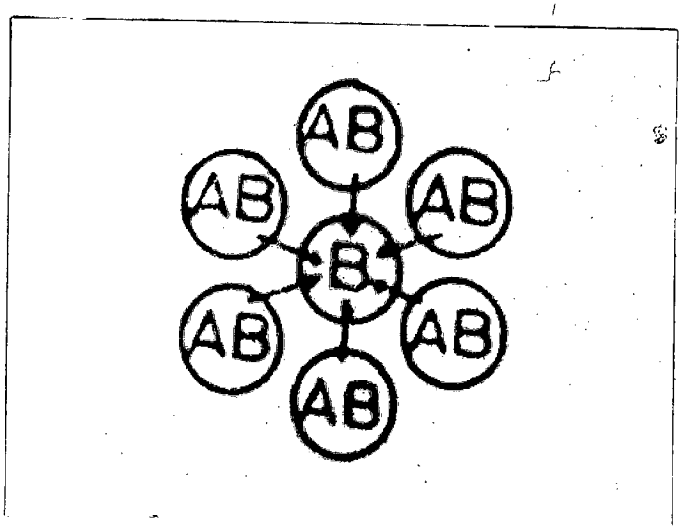

Fig. 9. - Propagation of the reaction in the individual grains.

the reaction, and (c) further reaction takes place by bulk diffusion of mobile reaction species through this product layer.

The equations of this category used to analyse the data are :

Jander[6]

$$K_j t = [1-(1-x)^{1/3}]^2 \quad \ldots \quad (4)$$

Kroger-Ziegler[37]

$$K_{kz} \ln t = [1-(1-x)^{1/3}]^2 \quad \ldots \quad (5)$$

Zhuravlev-Lesokhin - Tempol'man[38]

$$K_{ZLT} t = \left[\frac{1}{(1-x)^{1/3}} - 1\right]^2 \quad (6)$$

Ginstling-Brounshtein[39]

$$K_{GB} t = 1 - 2/3\, x - (1-x)^{2/3} \quad (7)$$

Valensi[40] - Carter[41]

$$K_{CV} t = \frac{z - [1+(z-1)x]^{2/3}(z-1)(1-x)}{z-1} \quad \ldots \quad (8)$$

Dunwald-Wagner[42]

$$K_{DW} t = \frac{6}{\ln \pi^2 (1-x)} \quad (9)$$

where x is fraction reaction completed, k is specific rate constant, t is reaction time, and z is volume of reaction product formed per unit volume of the reactant consumed.

II.5.2 PRODUCT GROWTH CONTROLLED BY NUCLEI - GROWTH

This approach considers the nucleation of the product phases at active sites and the rate at which the nucleated particles grow. The general form of the kinetic equation for nuclei - growth model is :

$$\ln (1 - x) = - (kt)^m \quad \ldots \quad (10)$$

where m is a parameter which is a function of (a) reaction mechanism (b) number of nuclei present (c) composition of parent and product phases (d) geometry of the nuclei.

II.5.3 PRODUCT GROWTH CONTROLLED BY PHASE BOUNDARY REACTIONS

When diffusion through the product layer is so rapid that the reactants cannot combine fast enough at the reaction interface to establish equilibrium, the solid - state reaction is phase boundary controlled. The product layer is discontinuous when the molar volume of the product phase is considerable less than that of the reactant on which it is growing. According to Laidler[43], when a discontinuous product phase occurs, the rate determining step may be the chemical process occuring at the phase boundary. Under these conditions the rate is determined by the available interface area, and such process are reffered to as topochemical. For a sphere reacting from the surface inward, the relation between fraction reaction completed and time is :

$$K_{PB}\, t = 1 - (1 - x)^{1/3} \quad \ldots \quad (11)$$

for a circular disc reacting from the edge inward, or for a cylinder

$$K_{PB}\, t = 1 - (1 - x)^{1/2} \quad \ldots \quad (12)$$

The two empirical relations are important in the field of ferrite forming reactions; first the Jander equation and secondly the Tammann equation.

JANDER'S EQUATION[4] : Previous kinetic studies on nickel ferrite and other ferrite system have been interpreted in terms of a model of the reaction developed by Jander, expressed by the Eq. (4). It is difficult to d educe the rate laws in most of the solid - state reactions. However, a simplified theoretical justification can be provided. Following assumptions were made in the derivation of Jander's equation.

(i) All reacting particles are of perfect spherical shape and uniform in size (described as A and B).

(ii) Particles A are surrounded by particles B. In the case of nickel ferrite, NiO (A) is completely surrounded by Fe_2O_3 (B).

(iii) Only particle B diffuses into A.

(iv) Only Fick's law of diffusion applies; other mechanisms are not considered.

(v) Both, particle size (r) and the constant k (associated with the diffusion constant) remains unchanged through the entire course of reaction.

and for a contracting cube :

$$X = 8k^3t^3 - 12k^2t^2 - 6kt \quad \ldots \quad (13)$$

II.5.4 PRODUCT GROWTH CONTROLLED BY KINETIC EQUATIONS BASED ON THE CONCEPT OF AN ORDER OF REACTION

Equations analogous to classical rate equations, mainly for expressing and correlating data, have often been applied to solid - state reactions. The integrated form of the general kinetic equation based on the concept of an order of reaction is :

$$\frac{1}{n-1}\left[\frac{1}{(1-x)^{n-1}} - 1\right] = kt \quad \ldots \quad (14)$$

where n is the so called order of the reaction. For certain values of n, Eq. (14) leads to some of the equations based on physical models. When n = 2/3 Eq. (14) is identical to Eq. (11); likewise when n = ½, Eq. (14) is identical to Eq. (12). When the rate determining step is the nucleation process and there is equal probability of nucleation at each active sites, one obtains by analogy with radioactive decay a kinetic equation of the first order. A t present, values of n other than ½, 2/3 and 1 leads to equations with no obvious physical significance. The general method for determining, if a reaction may be classified by a reaction order, is the van't Hoff differential analysis.

The two empirical relations are important in the field of ferrite forming reactions; first the Jander equation and secondly the Tammann equation.

JANDER'S EQUATION[4] : Previous kinetic studies on nickel ferrite and other ferrite system have been interpreted in terms of a model of the reaction developed by Jander, expressed by the Eq. (4). It is difficult to d educe the rate laws in most of the solid - state reactions. However, a simplified theoretical justification can be provided. Following assumptions were made in the derivation of Jander's equation.

(i) All reacting particles are of perfect spherical shape and uniform in size (described as A and B).

(ii) Particles A are surrounded by particles B. In the case of nickel ferrite, NiO (A) is completely surrounded by Fe_2O_3 (B).

(iii) Only particle B diffuses into A.

(iv) Only Fick's law of diffusion applies; other mechanisms are not considered.

(v) Both, particle size (r) and the constant k (associated with the diffusion constant) remains unchanged through the entire course of reaction.

Constant k in the Jander's equation is the slope of the $[1 - (1 - x)^{1/3}]^2$ vs t curve. The values of k over a temperature range may be used to find the activation energy Q of the Arrhenius equation :

$$k = A e^{-Q/RT} \quad \ldots \quad (15)$$

TAMMANN EQUATION[3] : - Jander's equation may be contrasted to an emperical expression derived by Tammann, which has been successfully applied to many ferrite systems. The Tammann equation is expressed as :

$$C = A \log t + B \quad \ldots \quad (16)$$

where C is the concentration of the reaction products, t is time, and A and B are constants. This logarithmic expression may be obtained by integration of Fick's laws of diffusion with the assumption that the concentration gradient is inversely proportional to time. By assuming that the concentration gradient, dc/dl, is inversely proportional to time, Fick's diffusion equation :

$$\frac{dx}{dt} = D \frac{dc}{dl} \quad \ldots \quad (17)$$

becomes

$$\frac{dx}{dt} = \frac{b}{t} \quad \ldots \quad (18)$$

where b is proportional to the coefficient of diffusion D. Integration gives the logarithmic rate law Eq. (15) where A is proportional to b.

The data available on ferrite systems have been analysed by both, the Jander's and the Tammann's expressions, by many workers. Jander's equation though excellent for many reactions appears to be somewhat limited in ferrite studies because the magnetic material formed can be in the completed and uncompleted stages in the final reaction. In the case of previous workers agreement with Jander's equation was poor. However, the treatment of data with Tammann's expression by Turnbull[44], Jaffercon[16] on Economos[10] on nickel ferrite was found satisfactory. Guillissen and van Rysselberghe[24] made a through study of zinc ferrite and found that the results were in accordance with the linear relationship (Tammann Law) for first three hours.

Blum en Li[11] in their study on nickel ferrite have shown that the oversimplified model of the reaction (Jander's relation) is far from being realised in practice. Therefore any conclusion based on Jander's equation will not represent the actual practice. If one differenciates Jander's equation with respect to time, one obtains :

$$\frac{dx}{dt} = K\left[\frac{3}{2}\,\frac{(1-x)^{2/3}}{1-(1-x)^{1/3}}\right] \quad \ldots \quad (19)$$

The inadequacies of Jander's equation may further be revealed by comparing the differenciated form with the reaction rate as evaluated from the experimental data. Blum an Li[11] in their experimental plots in Jander's form found that the predicted curve and the experimental curve do not agree very well, especially in the case of temperatures above 900°C, where the reaction is occuring very rapidly. However, it was found that the plots of xt versus 't' (Fig. 10) fit very well with the experimental results. From this plot they have also developed an expression for the rate of nickel ferrite reaction. The slope of the xt versus t curve may be given as :

$$\frac{d(xt)}{dt} = a \text{ (constant)} \quad \ldots \quad (20)$$

$$\text{or} \quad \frac{x\,dt + t\,dx}{dt} = a \quad \ldots \quad (21)$$

$$\text{or} \quad x + t\frac{dx}{dt} = a \quad \ldots \quad (22)$$

$$\text{or} \quad \frac{dx}{dt} = \frac{a-x}{t} \quad \ldots \quad (23)$$

Blum and Li[11] found Eq. (23) to fit very well with their experimental data. The validity of this equation was checked from the data of Frech[12] on magnesium ferrite,

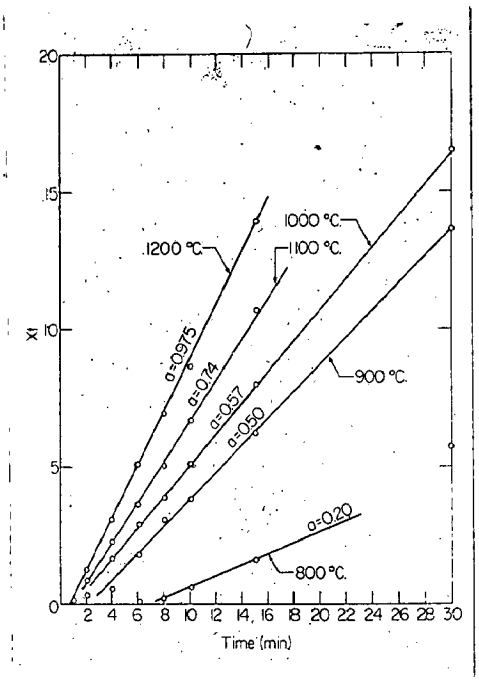

Fig. 10 - Plot of xt vs time of firing at various temperatures (dry mannual mixing) α = slope of curves[11].

and the data of Economos and Clevenger[10] on nickel ferrite system. The data were plotted in its orignal form, using Jander's equation and using Eq. (22) as xt versus t, for the sake of comparision. These plots are shown in Fig. 11A, 11B, 12A, and 12B. It was found that the Eq. (22) is well suited to represent rate of ferrite reactions.

The constant a in Eq. (22) is an isothermal reaction rate coefficient which includes all variables pertaining to the rate process. The constant a is closely related to the surface area ratio Fe_2O_3/NiO The constant a was essentially found independent of surface area at 800°C, where the reaction rate is slow. It increases, however, at other temperatures and probably reaches a maximum at an Fe_2O_3/NiO surface area ratio approaching unity.

Charp and Giess[45], however, have shown that the linear relation in Eq. (23) proposed by Blum and Li[11] does not hold, rather it is the curvature of the xt versus t plot. It has also been predicted that the neglection of the curve will be equivalent to the neglection of the reaction.

II. 6 FACTORS EFFECTING THE KINETICS OF FERRITE FORMATION

The important variables which affect the kinetics of ferrite formation are as follows :

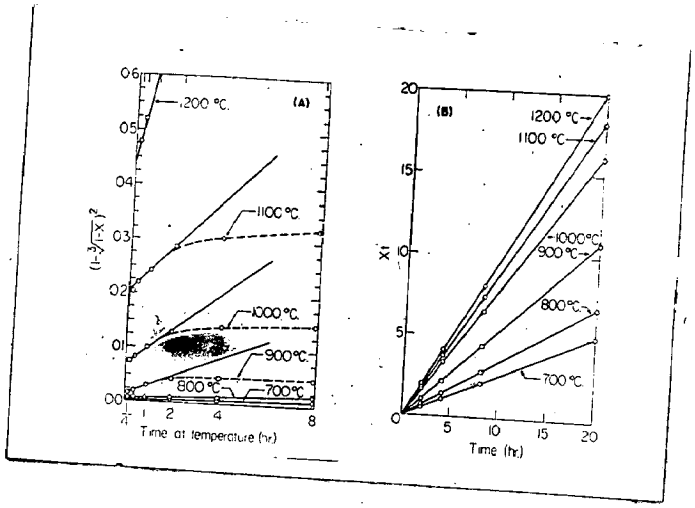

Fig. 11 - (A) Plot of $(1 - \underline{3}/\overline{1-x})^2$ vs time of firing for magnisium ferrite, and (B) plot of xt vs time for reaction of magnesium oxide and iron oxide[12].

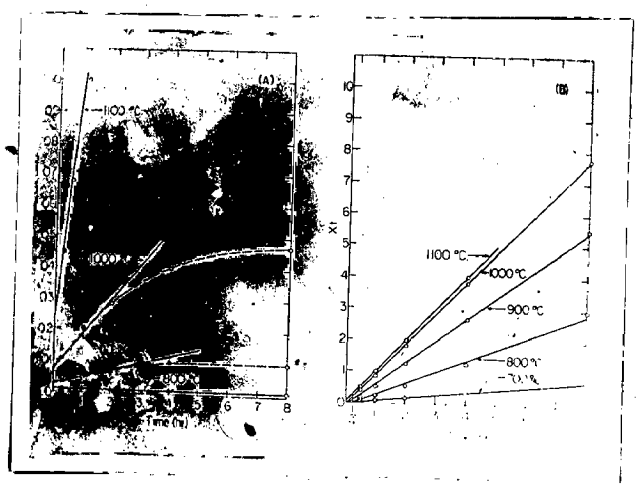

Fig. 12 - (A) Plot of $(1 - \underline{3}/\overline{1-x})^2$ vs time (B) plot of xt vs time for reaction of nickel oxide and iron oxide[10].

1. Particle size of the reacting oxides.
2. Particle shape of the reacting oxides.
3. Milling technique.
4. Temperature.
5. Oxygen partial pressure.
6. Trace impurities.
7. History of raw materials.

II.6.1 EFFECT OF PARTICLE SIZE

The particle size is of considerable importance to the industries. A great many oxide systems have been studied in the literature and the results of various experiments are not always comparable because of the variation in experimental techniques. Economos and Clevenger[10] have studied the effect of particle size of consistent oxides on the reaction kinetics of nickel ferrite. The results were analysed by the method derived by Jender[6] and more recently by Okamura and Shimoizaka[15] The activation energy for different iron oxide particle sizes were obtained. The results (Fig. 13) fall in the range of 50 kcal/mole for the mixture with the finest iron oxide to 70 kcal/mole for the coarsest particle.

With very fine particle factors associated with the surface may be expected to exert an influence on the reaction rate because of the increase in the

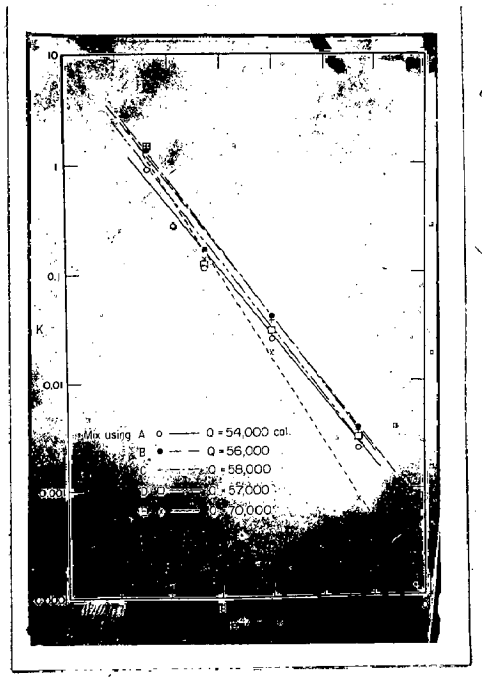

Fig. 13 - Activation energies of reaction of NiO with iron oxide[10].

surface/volume ratio. Blum and Li[11] have also studied the effect of particle size on nickel ferrite reaction and observed that the reactivity of different type of spherical shape α-Fe_2O_3 decreases with increase in the surface area ratio of α-Fe_2O_3 to NiO. This effect was found insignificant with the mixture used by Economos and Clevenger[10].

Frosh[12] studied the effect of particle size on reaction kinetics of magnesium ferrite. For a mixture of 0.03 - micron magnesium oxide and 0.05 - micron ferric oxide particles, reaction was observed after 15 minute at a temperature as low as 700°C while for coarse magnesium oxide particles (44 and 210 microns) and fine ferric oxide particles (0.05 micron), the initial reaction temperature increased to 1000°C. For coarse ferric oxide particles (44 and 210 microns) and fine magnesium oxide particles (0.03 microns), the reaction temperature was 900°C. The activation energies were 27.1 k cal/mole for the mixture of very fine components, between 116.2 and 118.5 for the fine ferric oxide and coarse magnesium oxide, and between 56.4 and 50.1 for the fine magnesium oxide and coarse ferric oxides. The effect of the varied particle size distribution of one of the constituents was not significant. For fine ferric oxide mixture, the variation could well be within the experimental error, but, for the fine magnesium oxide mixtures,

the reverse effect was noted; the finest of the ferric oxide gives the highest activation energy. This again might be within the experimental error.

II.6.2 EFFECT OF PARTICLE SHAPE

The particle shape of the consistent oxides also influence the reaction rate. It is observed that the mode of preparation of α- Fe_2O_3 appreciably effects the shape of Fe_2O_3 particles. Stephens[46] reported that spherically shaped Fe_2O_3 can be prepared by the calcinationof ferrous sulphate, acicular or needle shaped Fe_2O_3 by the dehydration of Fe_2O_3. H_2O crystals and cubical Fe_2O_3 by the high - temperature oxidation of Fe_3O_4. Blum and Li[11] examined this parameter on nickel ferrite, and observed that the acicular particles show the greatest degree of reaction throughout the entire temperature range, whereas, the cubical particles show the least degree. The acicular particles, being needle shaped probably have the greatest area of contact with the NiO particles.

II.6.3 MILLING TECHNIQUE

Blum and Li[11] has extensively studied the effect of milling technique on the kinetics of nickel ferrite formation, and observed that the type of milling method has also an effect on it. The milling methods

may be divided into two, dry and wet. Wet milling is more efficient than dry milling and it is very oftenly employed by ferrite manufacturers.

Three different milling methods were used by Blum and Li[11] during their study on nickel ferrite system. First is dry mechanical milling, in which a stochiometric amount of Fe_2O_3 and NiO were mixed and put into a steel ball mill loaded with steel pebbles and milled for 24 hours, in the dry state. Second is a dry manual mixing in which the weighed mixtures of reacting oxides were thoroughly mixed by passing it through a 50 - mesh sieve. And the last is wet milling of powder mixtures in ball mill in the presence of water, methyl alcohol or carbon tetrachloride. It was observed that mechanical milling and dry mixing are equivalent showing the approximate relative order of reactivity from various types of oxides. This is, however, not true in the case of wet milling. The effect of various milling liquids used is shown in Fig. 14.

Neeser and Scholz[47] have shown that mechanical distortion, such as milling, changes the lattic spacing of Fe_2O_3 and thus increases the reactivity. It may be seen from Fig. 14 that milling in water in porcelain mill with porcelain pebbles produces little or no magnetic material before firing of NiO and Fe_2O_3.

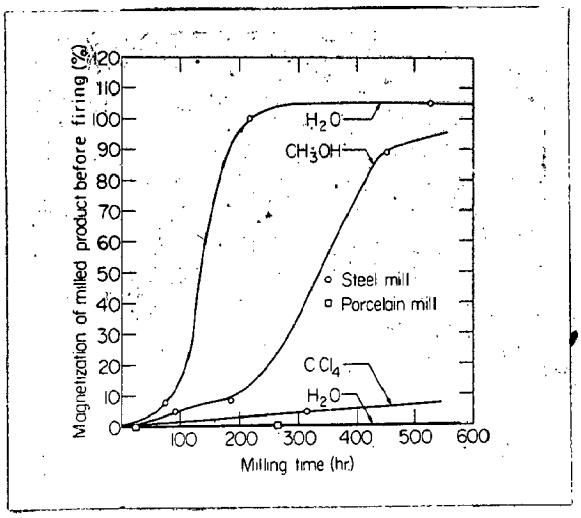

Fig. 14 - Effect of liquid media in milling[11].

However, milling in a steel mill with steel balls produces a great deal of magnetic material. This material no doubt comes from the wear of the mill and the balls, and probably some from the complex iron oxides. It has also been observed that the magnetic material formed is different in different milling liquids. Water shows the greatest reaction, methanol then next to the greatest, and carbon tetrachloride the least reaction. It may be predicted that the formation of magnetic products by the use of methanol and carbon tetrachloride as milling liquid is probably due to the presence of moisture which reacts with iron and leads to complicated results. It is not clear whether the polarity of the liquid would effect milling results or not. It has been observed emperimentally by Blum and Li[11] that on opening the mill a gas was found to escape. This shows that a gas is formed in the milling reaction.

II.6.4 TEMPERATURE

In diffusion controlled solid - state reactions temperature plays a significant role since the rate of diffusion is a function of temperature. For zinc ferrite, the exact point at which reaction between the two oxide components starts could not be determined accurately. However, measurable reaction

occured at 580°C after 1 hour, and above 600°C the reaction proceeds rapidly. The reaction reaches its completion below 1070°C. Kodes-dy and Katz[9] examined nickel ferrite and found that spinel formation occured at about 700°C, 100°C above that observed for zinc ferrite. The reaction reaches its completion at about 1200°C and the reaction kinetics was observed to increase with temperature.

Unlike the easy, gradual formation of spinel observed for zinc ferrite, nickel ferrite follows a more cumber-some pattern. At first, a few lines of the ferrite lattice appear, but high temperatures are needed for the rest of the diffusion pattern to appear. Kodesdy and Katz[9] have concluded that the initial diffusion process does not position the metal ions in their proper interstitial sites. The metal ions in both the nickel oxide rock - salt lattice and the ferric oxide corundum lattice occupy octahedral sites. To form the inverse spinel, repositioning of half of the ferric ions is needed plus the shift of the corundum oxygen lattice. The newly formed spinel lattice has the identical oxygen lattice of the nickel oxide, and it appears that some mutual solid - solution is possible at the new interface. This appears to interrupt the reaction until more elevated temperatures permit further diffusion and rearrangement.

Moore[17] in his study on magnesium ferrite obtained well defined plots at high temperatures e.g., 1301°C. and 1360°C. However, at low temperature e.g., 1155 and 1182°C, two well defined straight lines were observed with different slopes, indicating a higher reaction rate in the begining of the reaction. The changes in slope were observed after the thickness of the product layer of magnesium ferrite has reached a value approximately 10 μ at 1155°C and 100 μ at 1182°C. The high initial rate according to Kohn[48] is due to the formation of unstable solid - solutions, expanded or deformed lattices, crystallites of colloidal dimension and amorphous states. Tammann[49] has pointed out that the rate of removal of such defect sites is inversely proportional to time. One can also expect that an increase in temperature would have an even pronounced effect in the removal of such defects.

II.6.3 <u>OXYGEN PARTIAL PRESSURE</u>

When one of the reactants is a gas or when one of the product is a gas, the solid - state reaction kinetics would be a function of pressure. In the ferrite manufacture neither reactant nor product is a gas, However, the rate of ferrite formation is enhanced by the reduction of oxygen partial pressure of the surroundings. A recent study of the phase relationship in the Mg - Fe -O system has shown that at the reaction temperature of magnesium ferrite, ferric oxide is unstable near the ferrite

boundary and dissociates into magnetite and gaseous oxygen. Kooy[50] pointed out that the porosity observed during the solid - state reaction of ferrite is a direct result of the evolution of oxygen during the reduction of ferric oxide into magnetite.

Mason[51] dealt with the phase relationship of manganese ferrite and observed the appearance of spinel phase at 900°C. However, firing these same materials in an inert atmosphere (N_2 used here) produces the spinel much sooner, above 800°C. This shows that the ferrite forms at a lower temperature in an inert atmosphere than in the air. The chemistry of preparation of $MnFe_2O_4$ was discussed by Carter[52] with respect to oxygen content. Firing in air at 1300°C yields a single phase spinel. Changes in the oxygen content of the firing atmosphere will give rise to other phases.

II.6.6 TRACE IMPURITIES

The impurities present may effect the reaction kinetics of solid - state reaction in two ways. The reaction rate would become very fast when the liquid phase appears due to lowering of the eutectic point. If the eutectic point is not lowered below the reaction temperature, no significant change in rate is

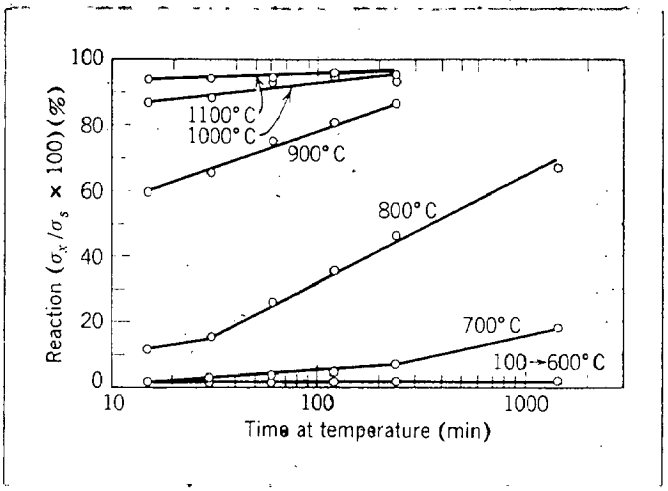

Fig. 15 - Reactivity of mixed oxides[56].

expected, provided the impurities do not affect the diffusion coefficient.

II.6.7 HISTORY OF RAW MATERIAL

It is apparent that the method of preparation of the reactants plays an important role in determining the reaction kinetics of solid - state reactions. The reacting oxides prepared by different chemical procedures have been found to give varying reactivity results. Hedvall[53] reported that ferric oxide prepared from ferric sulphate is more reactive than ferric oxide prepared from ferric oxalate. Economos and Clevenger[10] during their study on reaction rate of nickel ferrite from various specimen preparation techniques, noted that the oxalate mixtures of iron and nickel obtained by the coprecipitation method possess the highest reaction rate. Kido and Oziki[54] studied the relation between defect structure and reactivity for various nickel oxide prepared by different techniques, through electrical measurements. Bevan and Anderson[55] studied the same phenomina on zinc oxides prepared by various techniques. It has also been observed that the method of preparation effects the shape of $\alpha - Fe_2O_3$ formed, which has a direct influence on the reaction rate.

The location of the start of reaction between materials in the solid - state can be altered by the state of aggregation of the orignal components. This was concluded

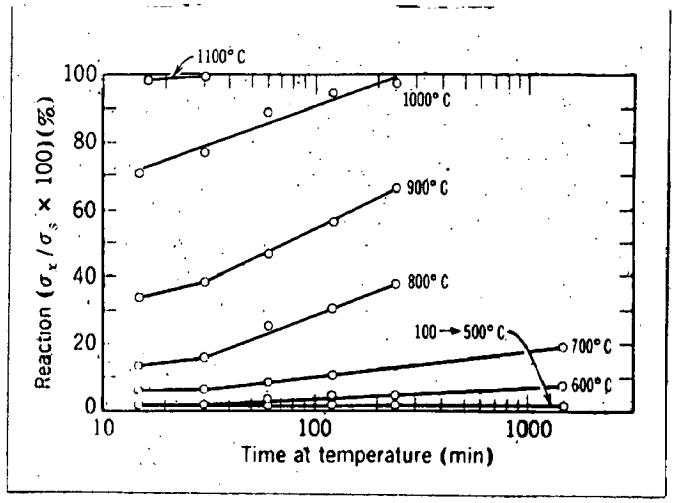

Fig. 16 - Reactivity of iron oxide - nickel carbonate[56] mixture.

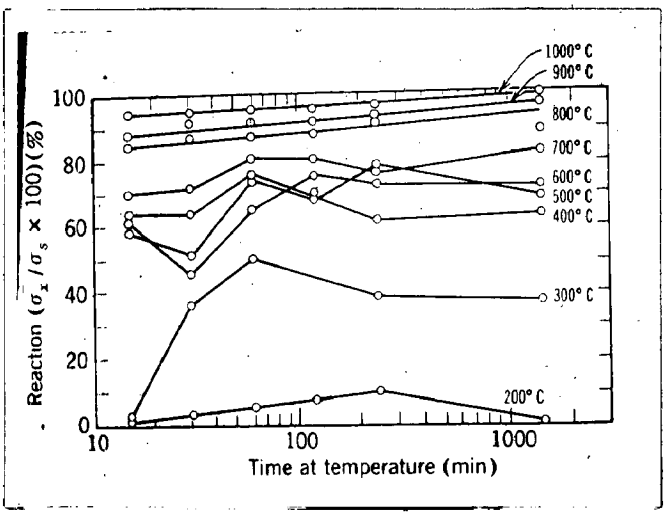

Fig. 17 - Reactivity of mixed crystal oxalate[56]

by Economos[56] by critically examining the various preparatory techniques. Fig. 15 shows the time and temperature dependence of ferrite formation for the mixed oxides. Magnetic - ferrite was observed at about 700°C. Okamura and Shiniozako[15] reported an activation energy of approximately 40 kcal for this reaction. With a mixture of nickel carbonate and iron oxide, the reaction follows a some what different pattern as shown in Fig. 16. Measurable reaction was found at 600°C. This decrease in reaction temperature can be attributed to the high reactivity of the newly formed nickel oxide from the carbonate decomposition. The oxalate reaction follows a rather erratic pattern, as seen in Fig. 17. Magnetite formation as an intermediate step can account for the gyrations observed. By holding for extended periods at a given temperature, this side effect can be over come.

****

CHAPTER III

****

EXPERIMENTAL WORK

III.1 MATERIALS USED

The following materials were used for the preparation of samples.

1. Ferric oxide precipitated BDH (London)
2. Nickel oxide NCI (India)

III.2 PREPARATION OF THE SAMPLES

Stochiometric amounts of ferric oxide (160 gram) and nickel oxide (75 gram) were weighed after drying thoroughly at 110°C in the oven for 5 hours. Wet mixing was carried out for 14 hours with the help of pestle and mortar. Water was used as a wetting agent. This was necessary to obtain intimate contact among the consituent oxides for getting the uniform results. The mixture was then dried in the furnace at low heat for 24 hours. The dried mixture was again ground in the pestle and mortar to get a uniform sized powder mixture.

Briquettes were prepared by compacting the powder mixture of 5 grams in a cylindrical die of 1.5 cm. internal diameter by applying a uniform pressure of 830 kg/cm^2. The briquettes were then heated in a furnace at 200°C to remove the moisture and the lubricant used on the die surface.

III.3 SINTERING OF THE SAMPLES

Pressed briquettes were sintered in air at eight different temperatures in an electric resistance furnace. The temperatures used for sintering were 700°, 800°, 850°, 875°, 900°, 930°, 1000° and 1100°C. The temperature was controlled in the range of $\pm 5^{\circ}$C. Sintering was carried out for 17 hours. Samples were taken out of the furnace after each hour.

The fired samples were again ground into powdered form, - 300 mesh size with the help of mortar and pestle for susceptibility measurements.

III. 4 SUSCEPTIBILITY MEASUREMENTS

Magnetic susceptibility measurements were carried out in the laboratory by Gouy's balance consisting of a semimicrometer balance for suspending and weighing the samples in a magnetic field of 700 gauses generated by an electromagnet. The method consists of the suspension of powdered sample in a cylindrical pyrex tube between the poles of an electromagnet as shown in Fig. 18. The sample should be suspended in such a manner that one end of the sample is in a region of larger field strength and the other in a region of negligible field. Correction was applied for the susceptibility of the glass. The accuracy of measurements on powdered

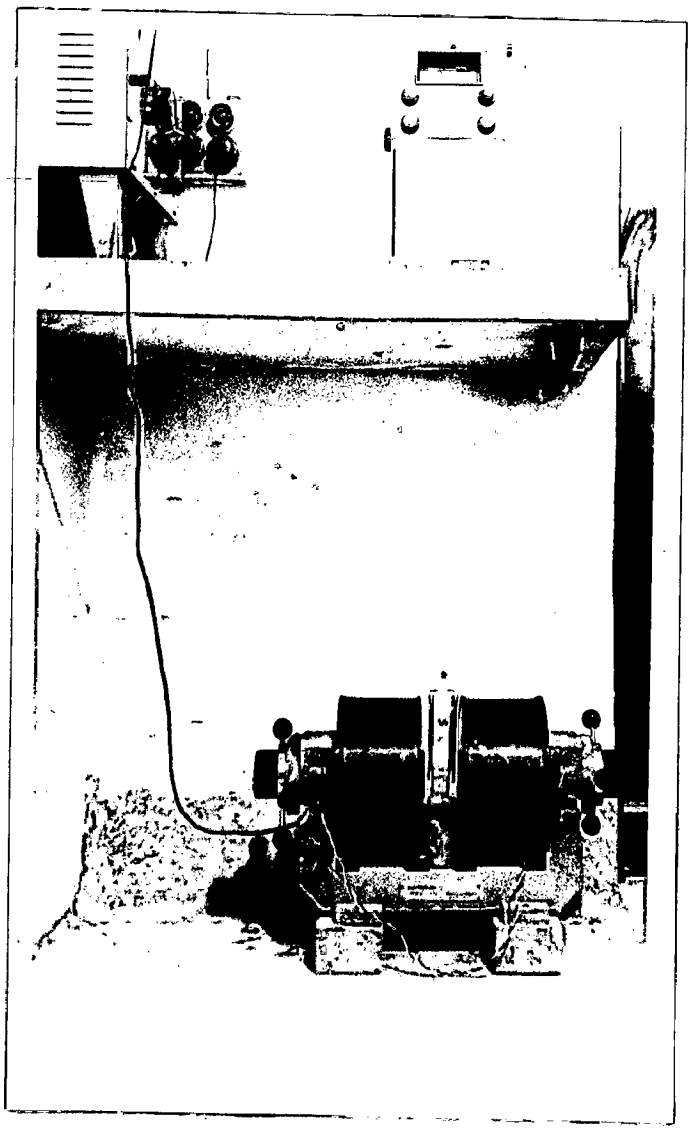

Fig. 18 - Apparatus for magnetic susceplibility measurement.

samples is severely limited by the uniformity and reproducibility of packing. It is difficult to exceed an accuracy of ± 1%. All observation were taken at room temperature i.e., 32°C.

The calculation of susceptibility has been carried out by the following formula :

$$S = C \frac{\Delta W}{W}$$

where C = the tube constant

W = the weight of the sample in grams.

ΔW = the change in weight on the application of the field in milli grams.

III. 5 CHEMICAL ANALYSIS

The chemical analysis of the fired samples was performed by dissolving the sample into dilute hydrochloric acid. Nickel oxide dissolves rapidly in a hydrochloric acid solution while ferric oxide and nickel ferrite either do not dissolve, or only dissolve slowly. One gram of the reacted samples were placed in 250 milliliters of dilute hydrochloric acid. The solution was heated to boil and was held for twenty minutes. The solution was filtered. Ammonium chloride and ammonium hydroxide were added to make the filterate alkaline. A small amount of

hydrochloric acid was added to make the solution just acidic.

The solution was boiled and 20 milliliter of 1% alcoholic solution of dimethyle glyoxime was added. The nickel in the solution preciptates as nickel dimethyle glyoxime. The preciptaties were filtered and transfered to a porcelain crucible. The praciptates were heated at about 120°C and weighed. The weight of dimethyle glyoxime multiplied by 0.2032 gives the weight of nickel in the leached solution. The concentration of nickel oxide in the leached solution could be related directly to the fraction of reaction completed.

CHAPTER IV

RESULTS AND DISCUSSION

IV.A. RESULTS

In the present investigation, the compacts of nickel oxide and ferric oxide were sintered at various temperatures, i.e., 700°, 800°, 850°, 875°, 900°, 1000° and 1100°C in air. The maximum time used for sintering was 17 hours. These compacts were then phase analysed by chemical and magnetic susceptibility measurement methods to obtain the fraction of reaction completed. The results obtained by magnetic analysis are given in Tables from 3 to 10 and they have also been plotted. Fig. 19 is the plot of susceptibility vs time at various temperatures. From the susceptibility values, fraction of ferrite formed were calculated and the results are plotted in Fig. 20. From this plot it can be seen that as the temperature is increased the rate of ferrite formation is also enhanced and the total nickel ferrite formed is much more at higher temperatures as compared with the low temperature values, for example at 1100°C the reaction is almost completed and about 96 percent of ferrite is formed after 17 hours sintering while at 700°C the amount of ferrite formed is only 27 percent. Therefore, the nickel ferrite formation is strongly temperature dependent reaction.

The specific reaction rate values were calculated with the help of the various rate equations developed by different workers. Viz., Jander[4], Kroger-Ziegler[37], Ginstling-

Figures from 22 to 25, the values of log of specific reaction rate constant (K) were then plotted against the reciprocal of the absolute temperature (Fig. 26 and 27). The values of activation energies found by various reaction models are listed in Table 16.

A comparision of the analysis results obtained by chemical and magnetic analyses are listed in Table 15.

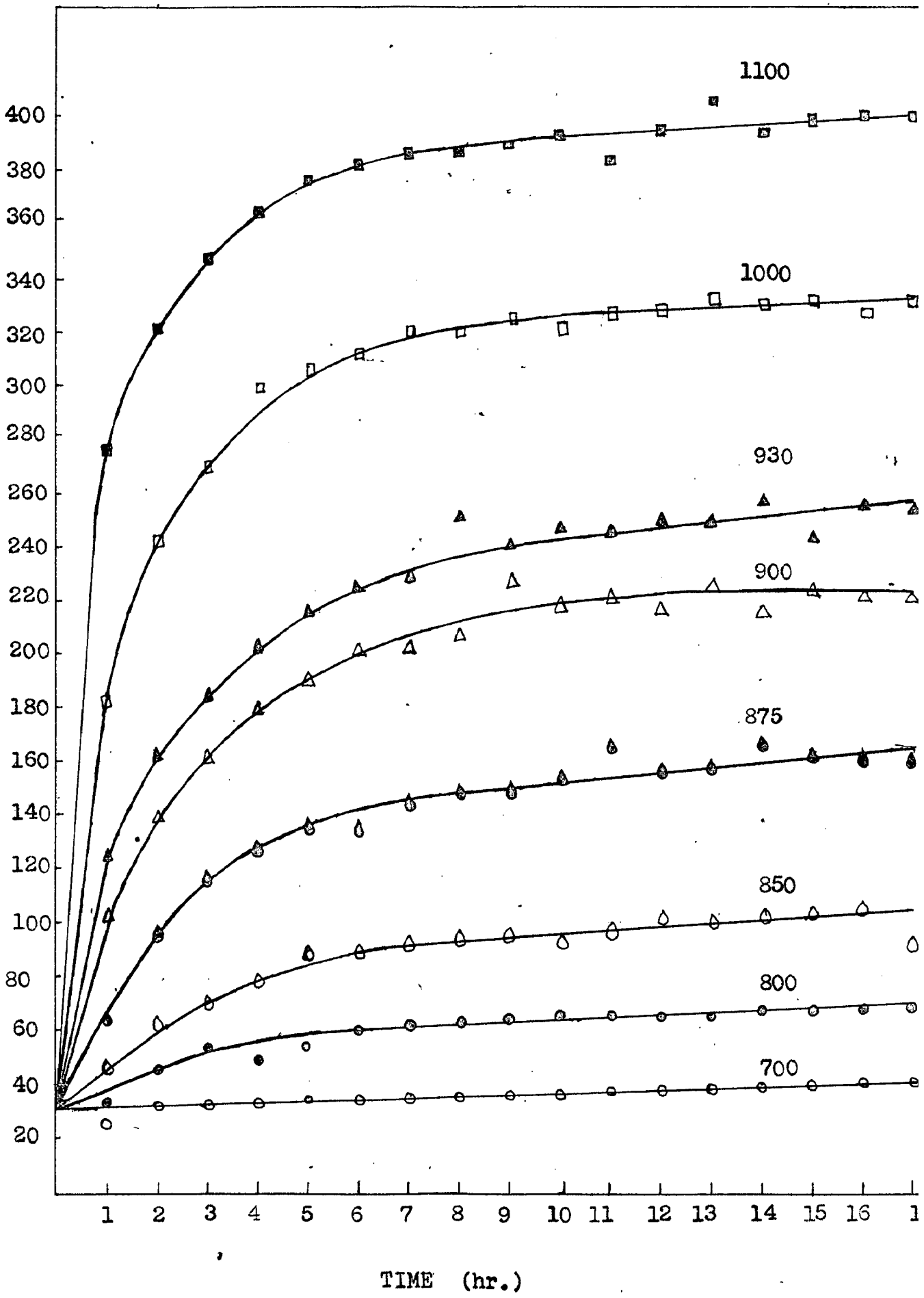

FIGURE 19 - PLOT OF SUSCEPTIBILITY VS TIME FOR SAMPLES FIRED AT VARIOUS TEMPERATURES.

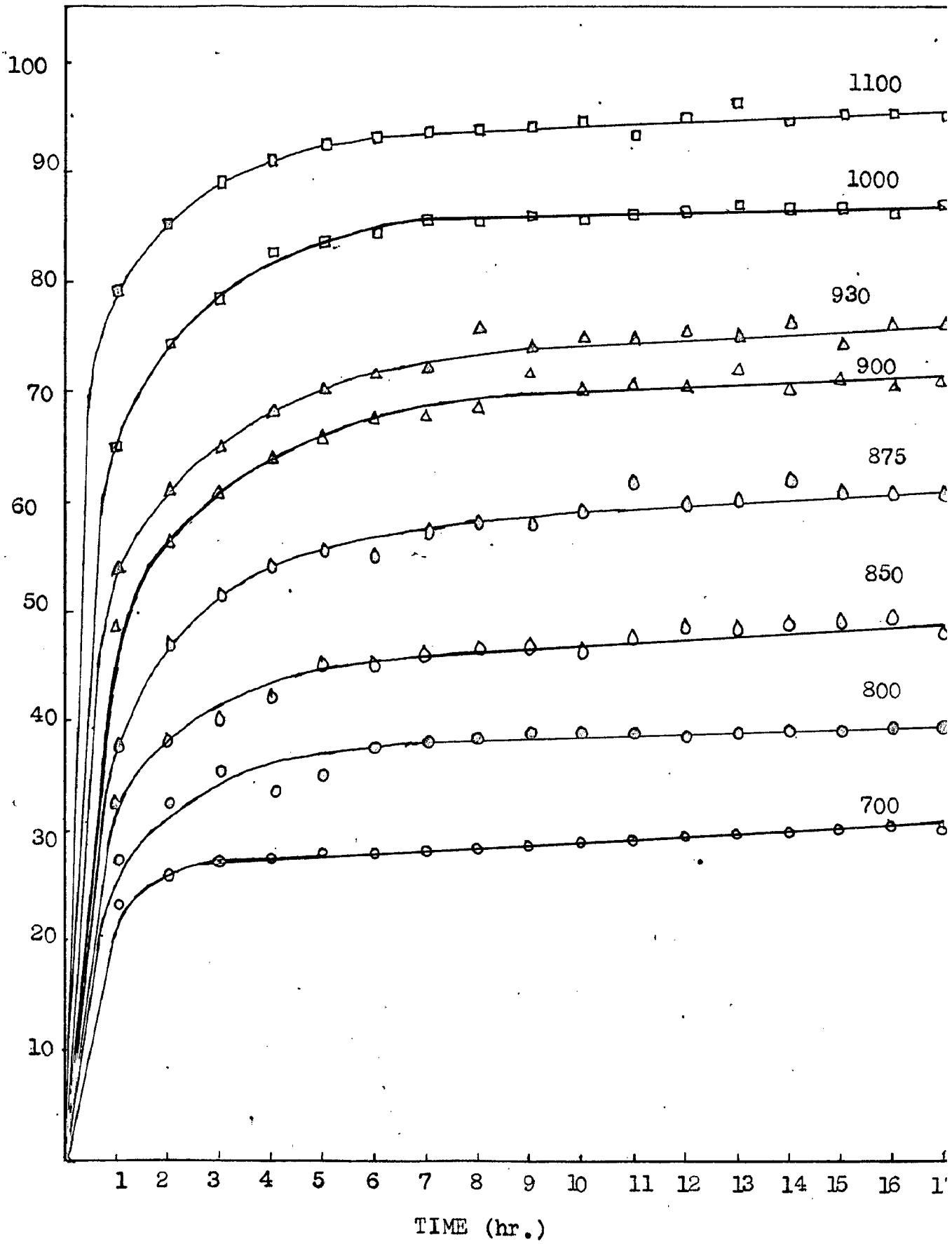

FIG. 20 - PLOT OF PERCENTAGE OF FERRITE FORMED VS TIME AT VARIOUS TEMPERATURES.

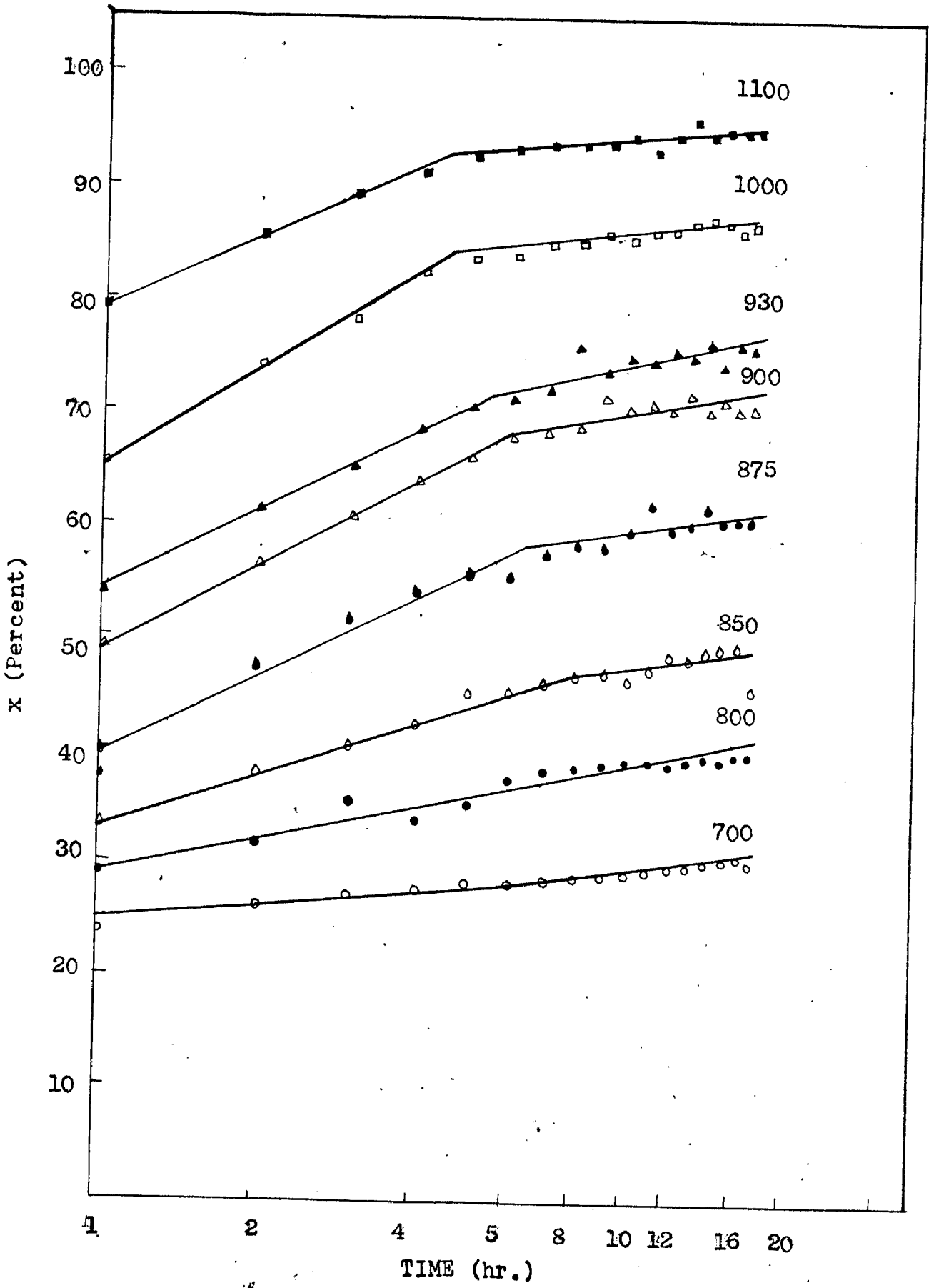

FIG. 21 PLOT OF FRACTION OF REACTION COMPLETED VS LOG t

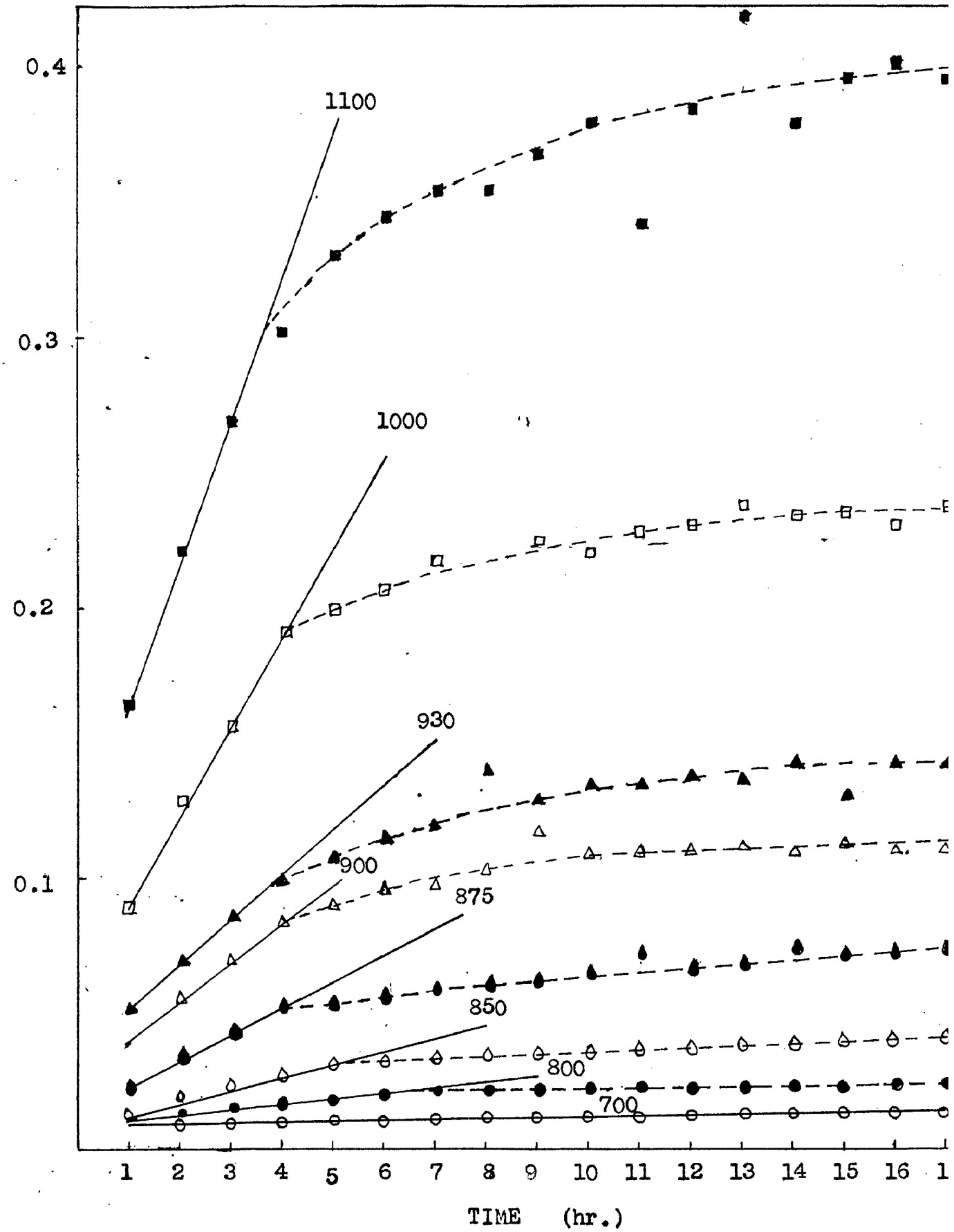

FIGURE 22 - PLOT OF $(1-(1-X)^{1/3})^2$ VS TIME AT VARIOUS TEMPERATURES

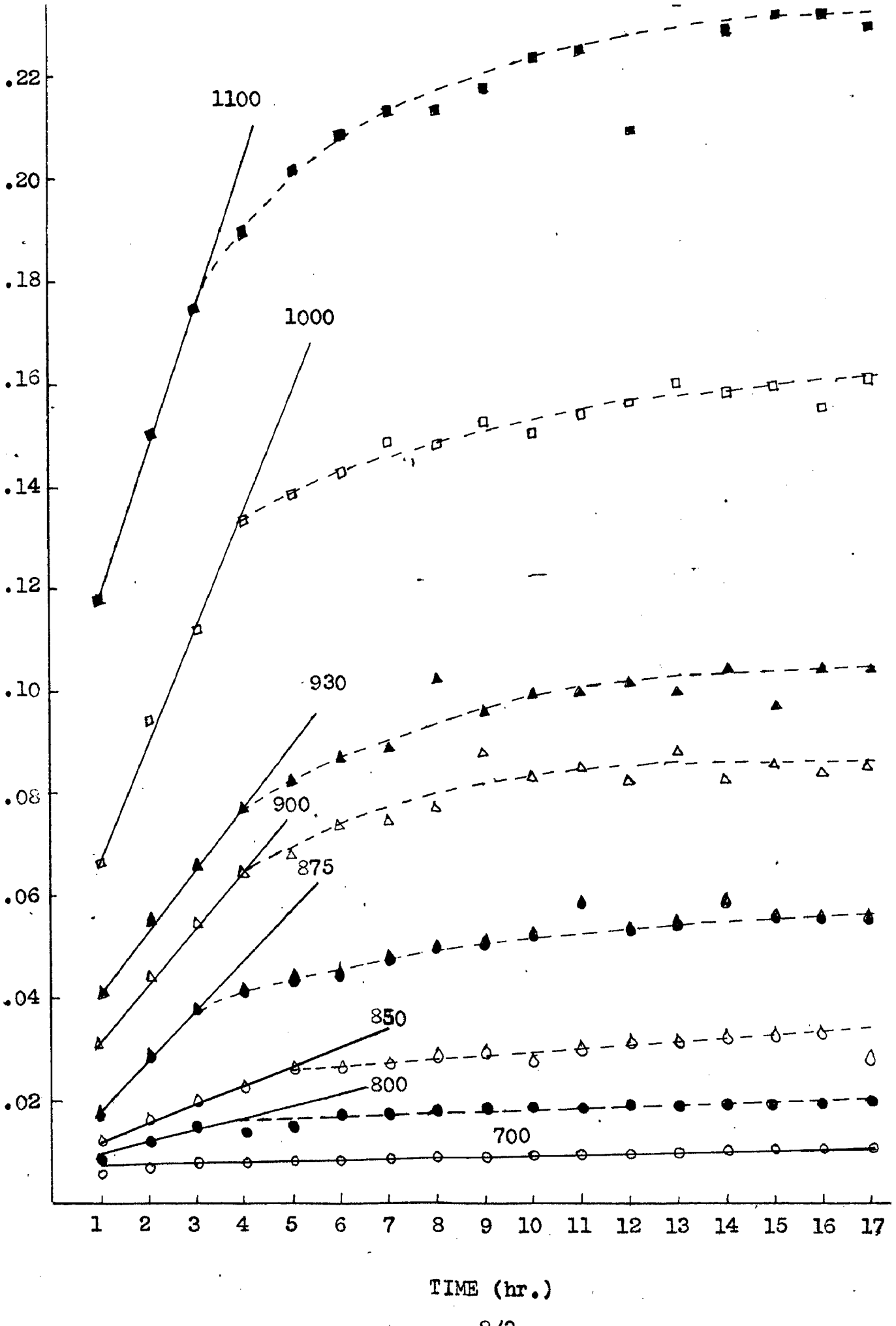

FIGURE 23 - PLOT OF $1-2/3Y-(1-Y)^{2/3}$ VS TIME AT VARIOUS TEMPERATURES

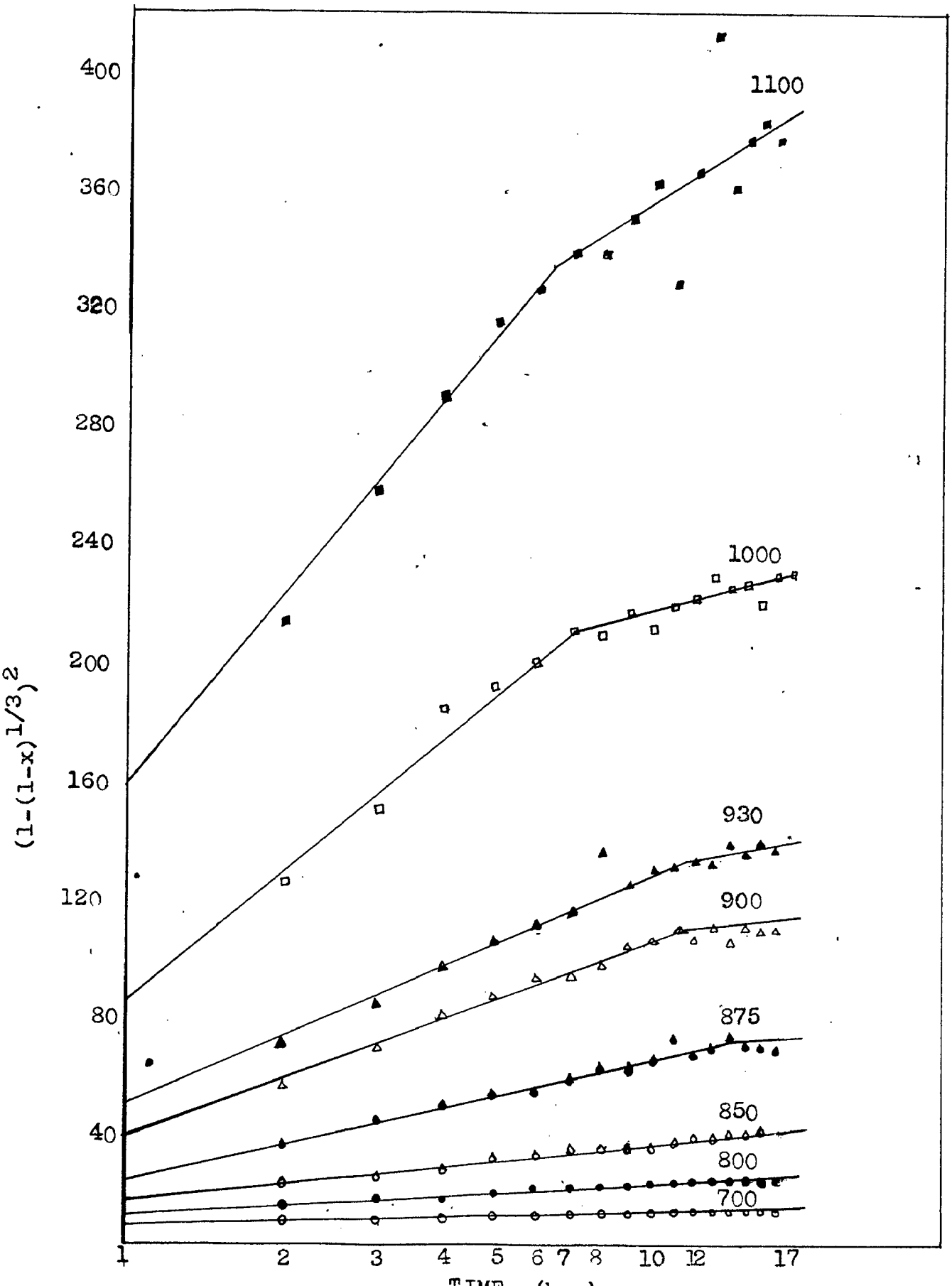

FIG. 24 - PLOT OF $(1-(1-x)^{1/3})^2$ VS LOG t AT VARIOUS TEMPERATURES.

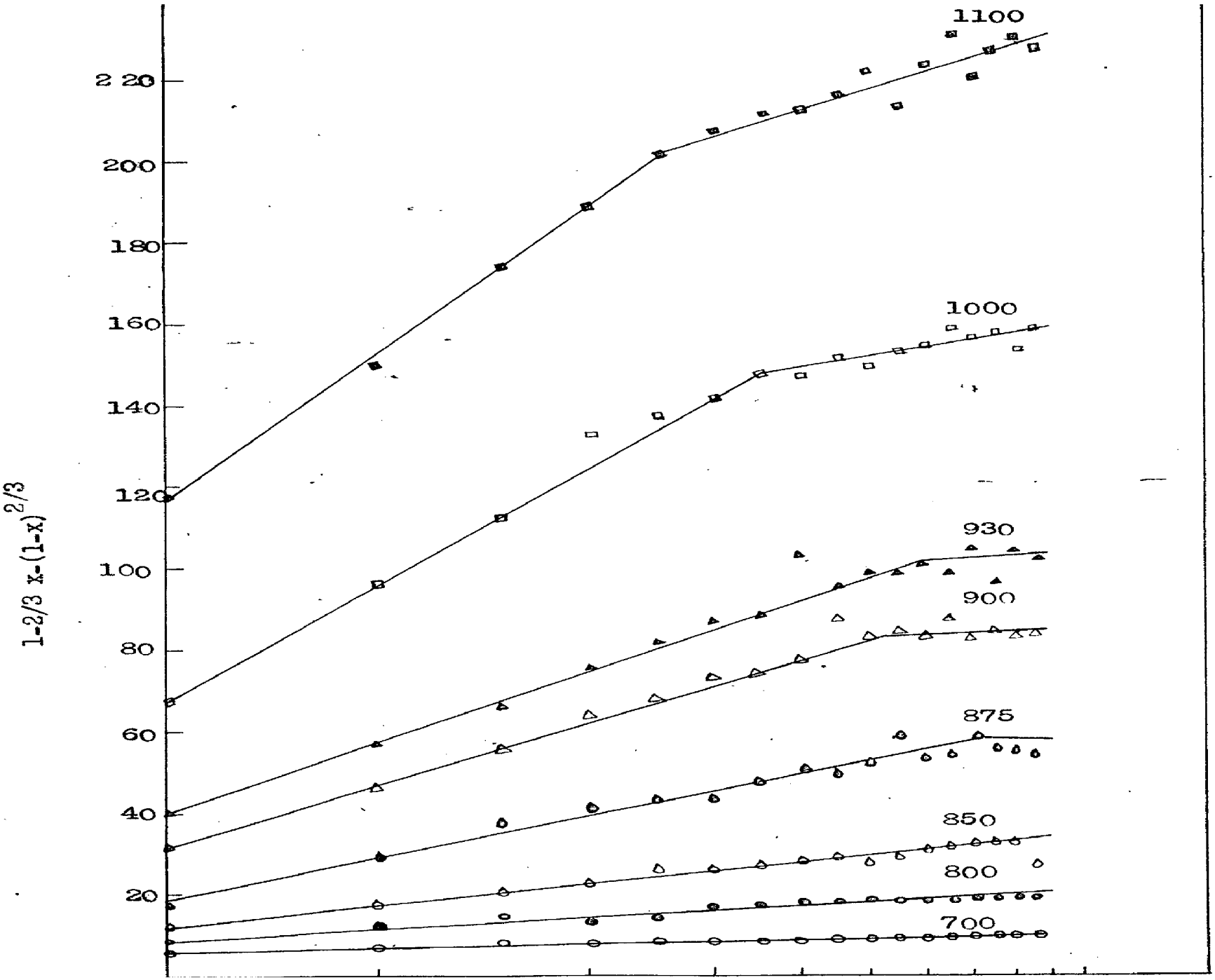
1100
1000
930
900
875
850
800
700
2 20
200
180
160
140
120
100
80
60
40
20
1-2/3 x-(1-x)^2/3

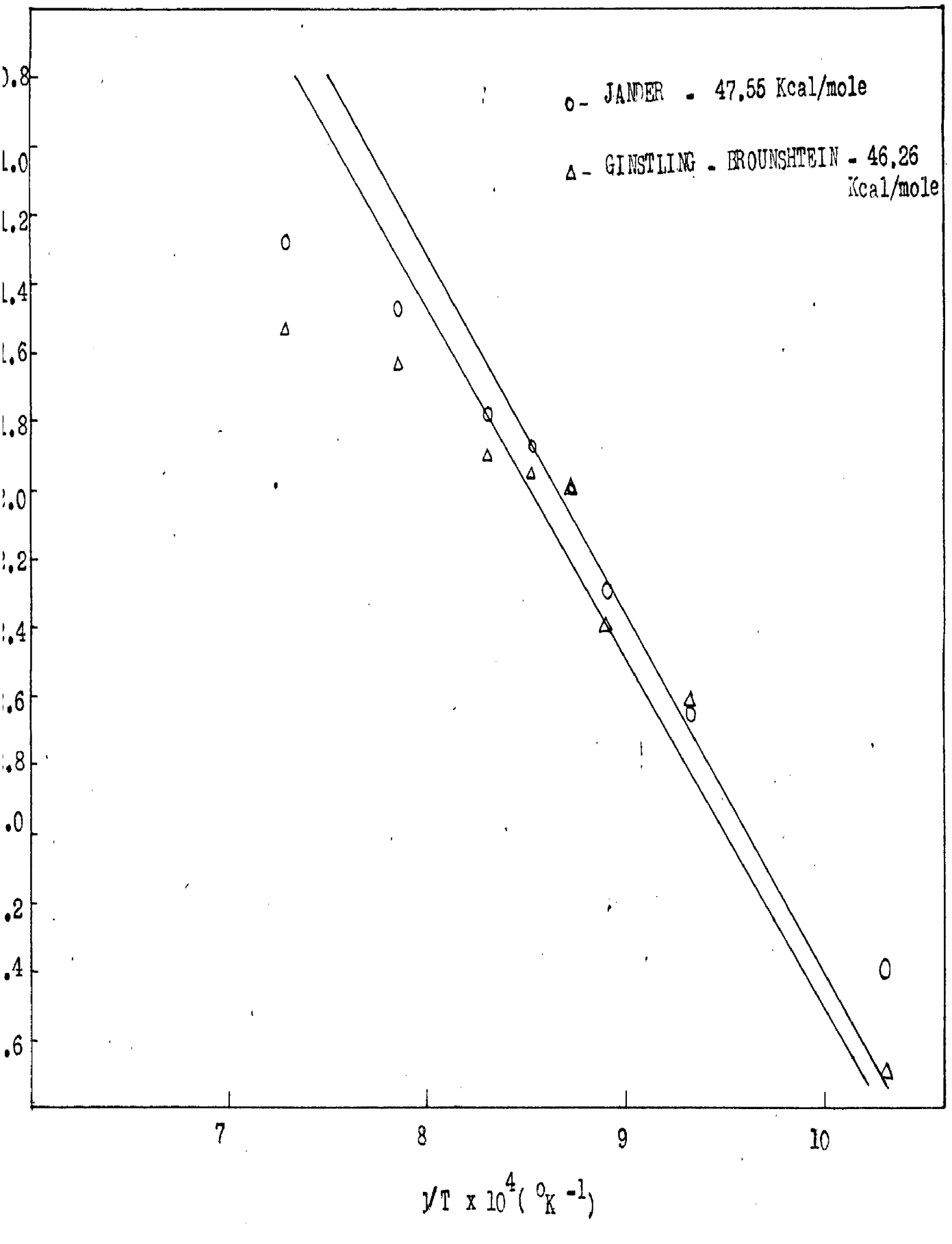
o- JANDER - 47.55 Kcal/mole
Δ- GINSTLING - BROUNSHTEIN - 46.26 Kcal/mole
0.8
1.0
1.2
1.4
1.6
1.8
2.0
2.2
2.4
2.6
2.8
3.0
3.2
3.4
3.6
7
8
9
10
y/T x 10^4 (°K^-1)

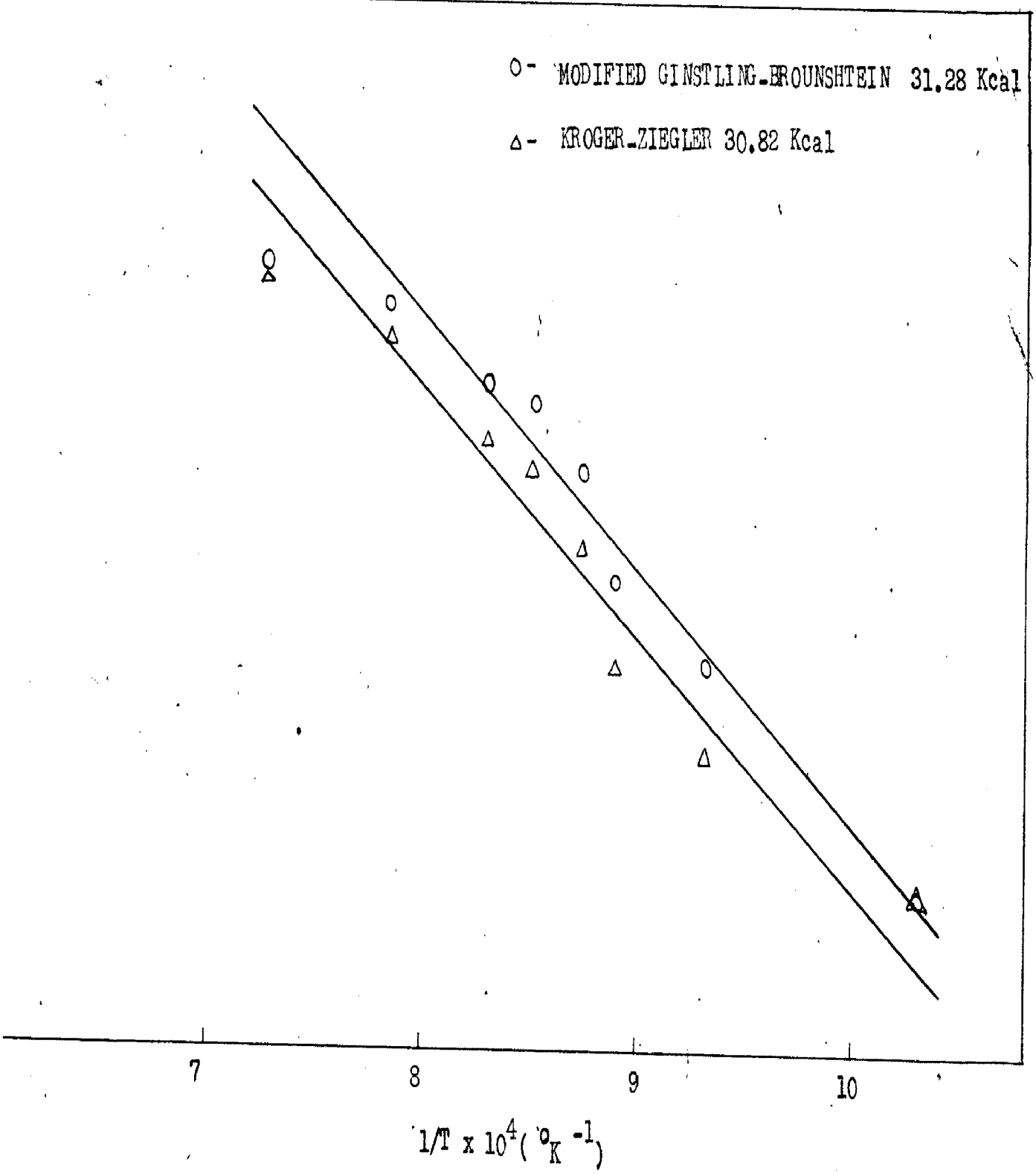

G. 27 - PLOT OF LOG K VS 1/T x 10^4 FOR KROGER - ZIEGLER AND MODIFIED GINSTLING - BROUNSHTEIN MODELS

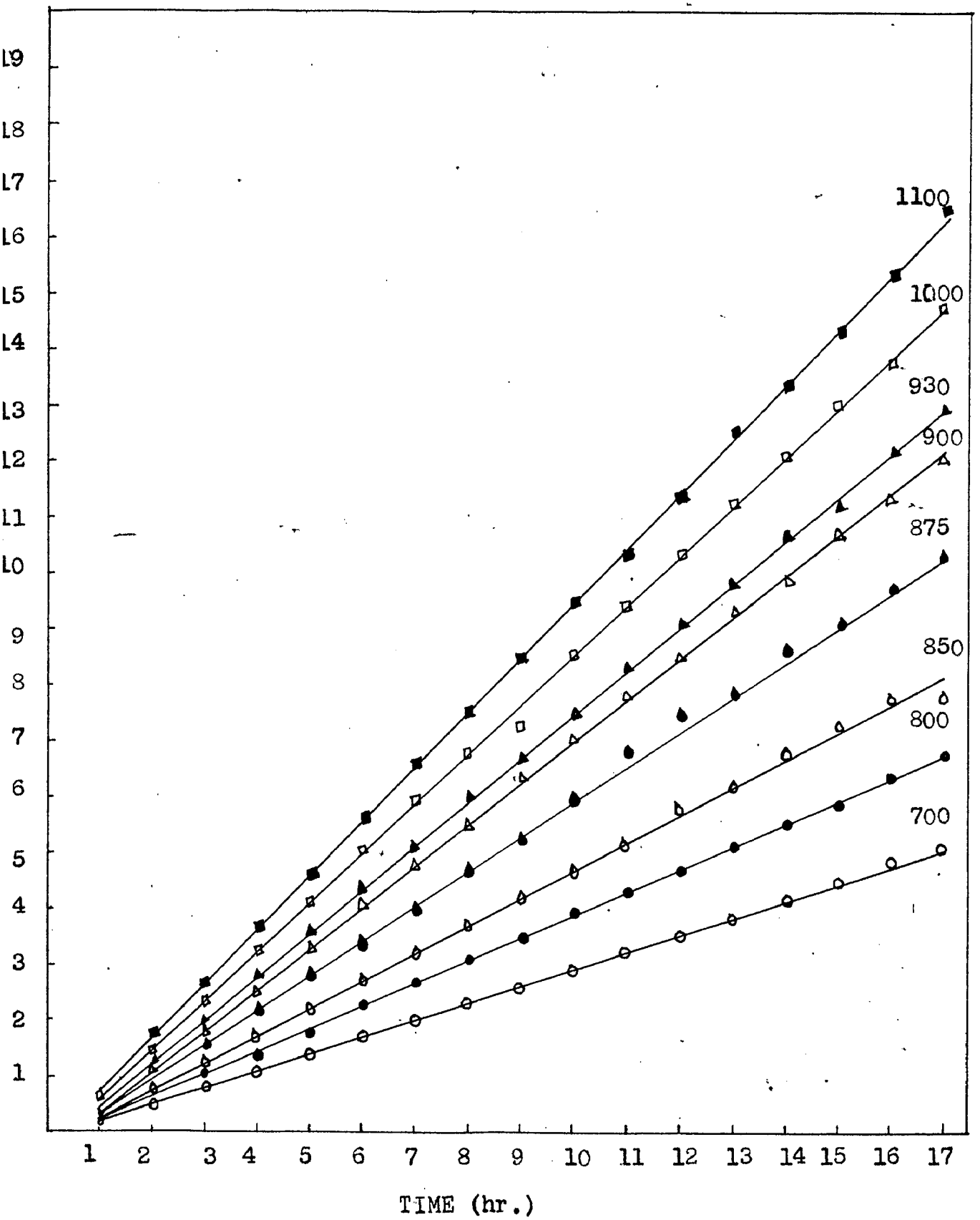

IG. 28 - PLOT OF xt VS TIME OF FIRRING AT VARIOUS TEMPERATURES

IV.2. DISCUSSION

The kinetics of ferrite formation depends on many variables, e.g., the properties of the reactants, the milling techniques and the presence of trace impurities[11]. A great many oxide systems have been studied and the results of various experiments are not always comparable because of the variation in experimental techniques. Hedvall[53] reported that ferric oxide prepared from ferric sulphate is more reactive than ferric oxide prepared from ferric oxalate. Economos and Clevenger[10] while studying the reaction rate from various specimen preparation techniques, noted that the oxalate mixture of iron and nickel obtained by the coprecipitation method possess the highest rate of reaction during nickel ferrite formation. The study of the kinetics of the formation of ferrite is thus complicated, because the various type of Fe_2O_3 and NiO are available and it is difficult to correlate the data of one set of experiment with the other. In the present study only one type of Fe_2O_3 and NiO were taken to minimise the effect of some of the variables discussed above. All samples were prepared under the same condition of milling, drying, and the pressure during compacting. This procedure also eliminated the effect of milling.

The formation of ferrite is a solid-solid type reaction (Eq.2). In such type of reactions the rate is generally controlled by the diffusion of reacting species through the product layer. Diffusion controlled reactions are very much influenced by the temperature and this is quite clear from the

..

present reaction data plots in Figs. 19 and 20. Appreciable reaction was observed at 700°C and the reaction seems to be completed at 1100°C when samples were fired for 17 hours.

The experimental data of the present investigation are analysed in terms of the model of the reaction developed by Jander,[4] Ginstling - Brounshtein[3], and Kroger - Ziegler[37]. The results are also analysed by the Tammann's[3] equation and the data plotted in Tammann's form are shown in Fig. 21. From this figure it can be seen that there are breaks in both the low as well as high temperature plots. The occurrence of such breaks in a fraction of reaction completed vs log time plots are an implication of a change in the mechanism of the formation of nickel ferrite. Hutting[57] has developed a model which explains these breaks in the formation of ferrite. According to him, various steps in the ferrite formation are as follows :

(1) Formation of surface layers of ferrite by the surface migration of one or both of the reactants.

(2) After acoherent surface layer of the ferrite is formed, bulk diffusion takes place.

(3) Completion of bulk diffusion and formation of final defect free bulk spinel in the mass.

The gradual formation of a defect free spinel structure during the nickel ferrite formation in the step-3 is supported by the x-ray analysis of Kedesdy and Katz[9], who have shown that the diffraction pattern from the samples sintered at low temperatures reveals partial completion of reaction where as the samples sintered at high temperature show higher degree of reaction completion in same time. Hutting[57] also calculated the activation energies for steps(1) and (2) for nickel ferrite formation and the values of activation energies reported were 30 and 13 K cal/mole, respectively.

There are two problems associated with the above interpretation of the mechanism of formation of nickel ferrite. The first is the high percentage of reaction product formed almost immediately upon the start of the reaction at temperatures above 800^{o}C, especially since a short time is required for the material to come to temperature in the furnace. The second problem is that the activation energy for bulk diffusion process is lower than that of the initial process attributed to surface diffusion. In determining the kinetics of solid-state reactions, the over all reaction rate may be determined by the time and conditions under which all the phases appear, by the diffusion rates of the species involved, and by the defect concentration of the reactants and product phases. It is this last condition which is believed to account for both the rapid formation of the reaction product and the lower activation energy in the second stage.

Since the degree of reaction was determined by magnetic susceptibility measurements, it is possible that a second magnetic phase in addition to nickel ferrite could contribute in a fictiously high percentage reaction. However, it should be noted that γ - Fe_2O_3 is relatively unstable at temperatures above 400°C, and also that no evidence for this component was found by x - ray analysis. In addition, the x - ray studies showed that the percent of nickel ferrite, for a reaction time, continuously increased as the reaction temperature was raised, thus accordingly satisfactory for a higher initial magnetization or percent reaction.

Since, it seems unlikely that the high, initial reaction can be explained on the basis of second magnetic component, an auxiliary mechanism must account for the fast reaction. the iron ion readily diffuses into the NiO lattice because of smaller ionic size (Table 17), and mechanism which would account for an enhanced diffusion would account for a fast initial reaction. It can be predicted that at higher temperatures a metastable or active nickel oxide is formed with a defect structure and, therefore, the activation energy for the iron diffusion would be expected to be low, giving rise to a faster reaction.

It is quite clear from Fig. 21 that not only one mechanism operates in the complete formation of nickel ferrite. This can also be seen from the plots of the reaction model developed by Jander[4], Ginstling - Brounshtein[39] and Kroger-Ziegler[37]. Jander's model is generally used to analyse the reaction rate of ferrite forming reactions and other solid - state reactions. The plots of reaction data in Jander's and Ginstling - Brounshtein's form show that these equations are applicable only in the initial stages of reaction. The activation energies calculated by Jander and Ginstling - Brounshtein reaction models are 47.55 and 46.26 K cal/mole, respectively. The activation energies calculated by these models are in good agreement. These equations are only applicable for a small duration of time. Therefore, the agreement of practical data with these equations are poor. This is also supported by the other workers[10,11]. It may be due to the geometrical-boundary conditions taken in the derivation of these models which are not met with the reaction of nickel ferrite formation.

The data were further analysed by the reaction models developed by Kroger - Ziegler[37], and modified Ginstling - Brounshtein, mathematically represented by equations (5) and (24), respectively.

$$1 - \frac{2}{3}x - (1-x)^{2/3} = K_{GB} \ln t \quad \ldots (24)$$

These curves also show the change in slope as is found in Tammann's plot. These equations better fit the experimental data than the Jander's and Ginstling-Brounshtein's equations. Although the geometrical - boundary conditions of the Jander's and Ginstling - Brounshtein's models are obviously not met, but the boundary conditions in these models coupled with the varying diffusion coefficient (as assumed in the derivation of Kroger - Ziegler and modified Ginstling - Brounshtein models) has proved a better mathematical representation of the nickel ferrite reaction.

The activation energies calculated by the application of Kroger - Ziegler and modified Ginstling - Brounshtein models are 30.82 and 31.28 K cal/mole, respectively, which are in good agreement. The values of activation energies calculated by Jander's and Ginstling - Brounshtein's reaction models are lower than that reported by Economos and Clevenger[10] and are in agreement with the values reported by Okamura and Shiniozaka[15]. This difference may be due to the different experimental conditions.

The experimental data of the present work were also analysed by the rate equation developed by Blum and Li[11] (Eq. 23). The plots of kt vs t are shown in Fig. 28. This shows that the equation proposed by Blum and Li[11] fits very well with the present reaction data on nickel ferrite. The validity of this equation was further checked by Blum and Li[11]

by plotting the data of Economos and Clevenger[10] on nickel ferrite and the data of Fresh[12] on magnesium ferrite.

CONCLUSIONS

On the basis of the results and discussion explained in chapter IV following conclusions can be drawn.

1. In the logarithmic plots (Tammann Law) change in the slope are observed at low as well as high temperatures which clearly indicates the change in the mechanism of nickel ferrite reaction.

2. The Jander's equation was reviewed and was found to be inadequate to describe ferrite forming reactions. The Ginstling - Brownshtein equation was also found unsatisfactory to describe the nickel ferrite reaction.

3. The Kroger - Ziegler and modified Ginstling - Brounshtein equations were revieved. These equations seem to fit the experimental data to a greater extent and essentially at lower temperatures these equations are obeyed. This may be due to the assumption of variable diffusion coefficient in the derivation of these models. At higher temperatures it also gives satisfactory results upto 7 hours of reaction.

4. The Arrhenius plots for the Jander, Ginstling - Brounshtein, Kroger - Ziegler and modified Ginstling - Brounshtein models have given the values of activation energies of 47.55, 46.26, 30.82 and 31.28 K. cal/mole, respectively.

5. Plot of data in the equation proposed by Blum and Li, (xt vs t) gives a straight line and fits the data very well.

****

REFERENCES

****

REFERENCES

1. Hilpert, S., Ber. deut. Chem. Ges., 42 , 2248 (1909).

2. Hedvall, J.A., Ber. deut. Chem. Ges., 45, 2095 (1912).

3. Tammann, G., Z.Anorg. u. allgem. Chem., 111, 78 (1921).

4. Jander, W., Z. anorg. u. allgem. Chem., 163. 1(1927).

5. Cobb, H.L., U.S.Patent 1, 946, 964, February 13,1934.

6. Kato, Y., and Takei, T., Trans. Am.Electrochem. Soc., 57 297 (1930).

7. Forestier, H., and Vetter, M., Compt. rend., 196, 164 (1939).

8. Economos, G., "Solid State Reaction in Ferrites", Kinetics of High - Temperature Processes, Kingery, W.D., John. Wiley and Sons, N.Y., (1959).

9. Kedesdy, H., and Katz. G., Ceramic Age 62, 29(1953).

10. Economos, G., and Clevenger, T.R., Jr., "Effect of Iron oxide Particle size on Nickel Ferrite Formation", J. Am. Ceram. Soc., 43 (1) 1148 - 52 (1960).

11. Blum, S.L., and Li, P.C., "Kinetics of Nickel Ferrite Formation", J. Am.Ceram. Soc., 44 (12) 611 - 17 (1961).

12. Fresh, D.L., "Study of Solid State Kinetics and Diffusion Phenomena of Reaction Between Magnesium Oxide and Ferric oxide at Elevated temperatures", Ph.D. Thesis, Catholic University of America, Washington, D.C., 1956.

13. Wagner, C., Z.Physik, Chem., B. 34, 309 (1936).

14. Economos, G., J. Am. Ceram. Soc., 38, 241 (1955).

15. Okamura, T., and Simizaka, J., Sci. Repts. Research Insts. Tohoku Univ. Az, 673 (1950).

16. Zafferson, C.F., Tech. Rept. 7, Department of Electrical Engineering, University of Michigan, Ann Arbor, Michigan, (January 1959).

17. Moore, W.L., and Venkatu, D.A., "Kinetics of Spinel Formation by Solid - state reaction in the System Mgo - Fe_2O_3", Trans, I.I.M. 23 , 77 (1970).

18. Chuforov, G.I., and Shchopetkin, A.A., etal, "Mechanism and Kinetics of Formation of Mg and Co Ferrites", Fiz. Fiz. Khim Svoistva Ferrtov, Mater. Dokl. vses, Soveshch., 4th. Minisk 1966, 25 - 31.

19. Fresh, D.L., and Dooling, J.S., J. Phys. Chem., 70 (1966) 3198.

20. Novrotsky. A. and Kleppa, O.J., J. Inorg. nucl. Chem., 30 (1968), 479.

21. Novrotsky. A. and Kleppa, O.J., Inorg, Chem., 5 (1966), 197.

22. Duncan, J.F. and Stewart, D.J., Trans. Faraday Soc., 63 (1967), 1031.

23. Rastogi, R.P., "Solid-Solid Reactions: Calssification, Mechanism of Interaction, Diffusion and Reaction Kinetics",

24. Guillissen, J., and Ryselberghe, R.J.V., Trans.Am. Electro Chem. Soc., 59, 95(1931).

25. Kedesdy, H.H., and Tauber, A., J.Am. Ceram.Soc., 39, 425 (1956).

26. Lindner, R., and Akerstrom, A., "Self Diffusion and Reaction in oxide and Spinel Systems", Z.Physik. Chem. (Frankfurt), (N.S.),6 (3/4) 162-77 (1956).

27. Hopkins, D.W., "Reaction Between Solids - Formation of Zinc Ferrite from Zinc Oxide and Ferric Oxide", J.Electro.Chem. Soc., 96(3) 195-203(1947) i Ceram Abstr., 1950, October p 211 b.

28. Paulus, M.P., and Eveno, P.Y., "Mechanism of Nickel Ferrite Formation", Reactivity of Solids,Mitchell, J.W., et.al., Wiley Interscience, 585,(1969),French.

29. Bengston, B and Jagitsch, R., Kemi Mineral. Geol., 26 (1) (1947), 14.

30. Branson, D.L., J.Am.Ceram.Soc. 48 (1965),591.

31. Yamaguchi . G. and Tokuda, T., Bull. Chem. Soc.Japan, 40 (1967), 0213.

32. Finch. G.I., and Sinha, K.P., "Electron-Diffraction Study of Transformation α- Fe_2O_3 to γ-Fe_2O_3", Proc.Roy. Soc.(London), AZ 41,1-8 (1957).

33. Nicholls, G.D., "Mineralogy of Rock Magnetism",Advances in Phys., 4 (14) 113-90 (1955).

34. Snoek, J.L., "Magnetic and Electrical Properties of the Binary Systems MO.Fe_2O_3," Physica, 3 (6)463 (1936); Cerem. Abstr., 17(3) 119(1938).

35. Mellor, J.W., A Comprehensive Treatise on Inorganic and Theoretical Chemistry.Longmans, Green and Company. London (1936).

36. DeBoer, F.S., Selwood, P.W., "Activation Energy for Solid-State Reaction γ-Fe_2O_3 = α-Fe_2O_3", J.Am.Chem. Soc., 76(13) 3365-67 (1956).

37. Kroger,C., and Ziegler, G., Ibid., 27,199(1954).

38. Zhuravlev, V.F., Lesokhin, I.G., and Tempel'man,R.G., Jour.Appl. Chem.USSR(English Transl.)21, 887(1948).

39. Ginstling, A.M., and Brounshtein, B.I., Jour.Appl. Chem. USSR (English Transl.) 23, 1327 (1950).

40. Velonsi, G., Compt. Rend., 202, 309 (1936).

41. Carter, R.E., Jour. Chem. Phys. 34, 2010(1961).

42. Dunwald.H., Wagner, C., Z.Physik. Chem. (Leipzig) B24, 53 (1936).

43. Laidler, K.J., Ibid 316, "Chemical Kinetics",McGraw-Hill Inc. New York (1965).

44. Turnbull. R.C., "Reinterpretation of the Reaction Kinetics of Nickel Ferrite", J.of Applied Physics, Supplement to Vol. 32, No.3, Mar. (1961).

45. Charp, S.H., and Giess, E.A., "Comment on Kinetics of Nickel Ferrite Formation", J.Am.Ceram.Soc. 54 (4), 200 (1962).

46. Stephens, R.A., "Iron Oxides as raw Materials for Manufacturer of Magnetic Ferrites", Am-Ceram.Soc. Bull., 38 (3) 106-109 (1959).

47. Naeser, G., and Scholz, W., "Effect of Mechanical Treatment on Reactigity of Solids", Kolloid-z., 156(1) 1-8 (1958); Ceram.Abstr., 1960, May. p.126b.

48. Kohn.C., Chem. Rev., 42 (1948) 527.

49. Tammann, G., Z.Anorg. Allgem.Chem 149 (1925).

50. Kooy.C. Proc. of 5th International Symposium on Reactivity of Solids, Elsevier Publishing Co., 1965, p 21.

51. Mason, B., Am. Mineralogist, 32, 426 (1947).

52. Gorter, E.W., Proc. I.R.E., 43, 1945 (1955).

53. Hedvall, J.A., Introduction to Chemistry of Solids, Vol. VCI.Friedrich Vieweg and Sohn, Braunsthweight1952.

54. Iida, Y. and Ozaki, S., Sintering of High-Purity Nickel Oxide, II", J.Am.Ceram. Soc., 42 (5) 219-28 (1959).

55. Bevan, D.J.M., and Anderson, J.S., "Electronic Conductivity and Surface Equilibria of Zinc Oxide", Discussions Faraday Soc., 1950, No.8, 238-41.

56. Economos, G., "Evaluation of Some Methods of Nickel Ferrite Formation", J.Am.Ceram. Soc. 42 (12) 628-32 (1959).

57. Hutting, G.F., Handbuch der Katalyse edited by G.M.Schwab (Springer-Verlag, Vienna, 1943), Vol.VI P.318.

58. Goldschmidt, V., Trans.Faraday Soc. 25:293 (1929).

****

APPENDIX A

****

TABLE 1

LATTICE ENTROPIES OF FORMATION (ΔS°_{298}) OF SPINELS

(The lattice entropy values are in e.u.)

Spinel	AB_2O_4 (S°_{298})	AO (S°_{298})	B_2O_3 (S°_{298})	ΔS°_{298}
$CoFe_2O_4$	32.2	10.5	21.5	+0.2
$ZnFe_2O_4$	35.0	10.4	21.5	+4.1
$CuFe_2O_4$	32.3	10.4	21.5	+0.4
$MgFe_2O_4$	28.2	6.4	21.5	+0.3
$NiFe_2O_4$	30.1	9.2	21.5	-0.6

TABLE - 2

ENTHALPY CHANGES IN SOLID STATE REACTIONS

Reaction	ΔH kcal/mole	Temp. $^{\circ}K$
$CoO+Fe_2O_3 = CoFe_2O_4$	-5.89 ± 0.21	970
$MgO+Fe_2O_3 = MgFe_2O_4$	-4.43 ± 0.24	970
$NiO+Fe_2O_3 = NiFe_2O_4$	-1.22 ± 0.22	970
$CuO+Fe_2O_3 = CuFe_2O_4$	$+5.05\pm0.20$	970

TABLE 3 - EXPERIMENTAL DATA FOR THE SAMPLES FIRED AT 700°C.

S.N.	Time (hr.)	Weight of the tube + Nickel Ferrite + Field off (grms)	Weight of the tube + Nickel Ferrite + Field on. (grms)	Susceptibility 10^{-6} (cgsm)	Bohr Magneton	Fraction of Ferrite formed (x)	$(1-(1-x)^{\frac{2}{3}})^2$	$1-2/3x-(1-x)^{\frac{2}{3}}$
1	1	10.66700	10.70080	26	3.76	.235	.007	.005
2	2	10.55215	10.58170	30	4.16	.260	.009	.007
3	3	10.58035	10.61535	32	4.32	.270	.010	.008
4	4	10.61780	10.65940	33	4.40	.275	.010	.008
5	5	10.56315	10.59900	35	4.49	.281	.011	.008
6	6	10.56230	10.60900	36	4.48	.280	.011	.008
7	7	10.59845	10.63910	35	4.53	.283	.011	.008
8	8	10.59330	10.63390	36	4.56	.285	.011	.009
9	9	10.58300	10.62260	36	4.57	.286	.011	.009
10	10	10.62760	10.67435	37	4.65	.291	.012	.009
11	11	10.66230	10.71420	38	4.69	.293	.012	.009
12	12	10.57250	10.61325	38	4.72	.295	.012	.009
13	13	10.59280	10.65010	39	4.78	.298	.022	.010
14	14	10.63225	10.68260	39	4.80	.300	.012	.010
15	15	10.64215	10.69480	40	4.83	.302	.013	.010
16	16	10.65100	10.70570	41	4.88	.305	.013	.010
17	17	10.63270	10.68310	40	4.80	.300	.0129	.010

Weight of the empty tube = 10.26480 grms.

TABLE 4 - EXPERIMENTAL DATA FOR THE SAMPLES FIRED AT 800°C

S.N.	Time (hr.)	Weight of the tube +Nickel Ferrite + Field off (gms.)	Weight of the tube +Nickel Ferrite + Field on. (gms.)	Susceptibility 10^{-6} (cgsm)	Bohr Magneton	Fraction of Ferrite formed (x)	$(1-(1-x)^{1/3})^2$	$1-\frac{2x}{3}-(1-x)^{2/3}$	
1	1	10.62020	10.66585	33	4.41	.276	.010	.008	.
2	2	10.58530	10.63715	47	6.21	.326	.015	.012	.
3	3	10.58035	10.64090	55	5.68	.355	.018	.015	1.
4	4	10.61780	10.67775	49	5.34	.334	.016	.013	1.
5	5	10.56315	10.61880	45	5.60	.350	.018	.014	1.
6	6	10.56230	10.62595	62	6.00	.375	.021	.017	2.
7	7	10.59330	10.66590	64	6.09	.381	.021	.017	2.
8	8	10.61785	10.69750	65	6.16	.385	.022	.018	3.
9	9	10.62400	10.70630	66	6.20	.388	.022	.018	3.
10	10	10.61335	10.69545	68	6.28	.393	.023	.019	3.
11	11	10.59300	10.66895	67	6.24	.390	.023	.018	4.
12	12	10.62325	10.70410	65	6.16	.385	.022	.018	4.
13	13	10.64500	10.73210	66	6.20	.388	.022	.018	5.
14	14	10.61110	10.69210	68	6.27	.392	.023	.019	5.
15	15	10.62050	10.70285	67	6.24	.390	.023	.018	5.
16	16	10.65300	10.74565	69	6.33	.396	.023	.019	6.
17	17	10.63605	10.74890	69	6.32	.395	.023	.019	6.

TABLE - 5 :- EXPERIMENTAL DATA FOR THE SAMPLES FIRED AT 850°C

Time (hr.)	Weight of the tube + Nickel Ferrite + Field off (grms)	Weight of the tube + Nickel Ferrite + Field on. (grms)	Susceptibility 10^{-6} (cgsm)	Bohr Magneton	Fraction of Ferrite formed (x)	$(3-(1-x))\,1/3^2$	$1-\frac{2}{3}x-(1-x)^{2/3}$	$N^{\#}$
1	10.66085	10.724650	46	5.20	.324	.015	.012	.324
2	10.65090	10.73570	63	6.08	.380	.021	.017	.760
3	10.67600	10.77610	70	6.40	.400	.024	.020	1.200
4	10.62840	10.72650	78	6.73	.421	.027	.022	1.684
5	10.62220	10.73235	89	7.20	.450	.032	.026	2.250
6	10.61140	10.71775	89	7.81	.449	.032	.026	2.694
7	10.60345	10.71250	93	7.36	.460	.034	.027	3.220
8	10.61960	10.73635	95	7.44	.465	.035	.028	3.720
9	10.62355	10.74260	96	7.47	.467	.035	.029	4.203
10	10.63345	10.75220	93	7.36	.460	.034	.027	4.600
11	10.65095	10.78130	97	7.53	.471	.036	.029	5.181
12	10.67570	10 .8228	103	7.76	.485	.039	.031	5.820
13	10.67530	10.81925	101	7.68	.480	.038	.031	6.240
14	10.60340	10.72560	104	7.79	.487	.039	.032	6.818
15	10.65090	10.79200	105	7.84	.490	.040	.032	7.350
16	10.63500	10.76970	105	7.82	.489	.039	.032	7.824
17	10.70005	10.83420	89	7.20	.450	.032	.026	7.650

TABLE 6 - EXPERIMENTAL DATA FOR THE SAMPLES FIRED AT 875°C

Time (hr.)	Weight of the tube +Nickel Ferrite + Field off (grms.)	Weight of the tube +Nickel Ferrite + Field on. (grms.)	Susceptibility 10^{-6} (cgsm)	Bohr Magneton	Fraction of Ferrite formed (x)	$(1-x-y)^{1/3}$	$1-\frac{2}{3}x-(1-x-y)^{2/3}$	$\frac{1}{2}x$
1	10.74650	10.84720	62	6.00	.375	.021	.017	.375
2	10.71140	10.86155	97	7.52	.470	.032	.029	.940
3	10.76125	10.96240	117	8.25	.516	.045	.037	1.548
4	10.70605	10.90190	128	8.64	.540	.051	.041	2.160
5	10.73790	10.95730	134	8.83	.552	.054	0043	2.760
6	10.77705	11.01290	133	8.80	.550	.054	.043	3.300
7	10.71625	10.94028	143	9.13	.571	.059	.047	3.997
8	10.70500	10.93190	149	9.31	.582	.063	.050	4.656
9	10.78605	11.05290	148	9.28	.580	.062	.0049	5.220
10	10.74650	11.00430	155	9.48	.593	.066	.052	5.930
11	10.75520	11.04210	169	9.92	.620	.075	.059	6.820
12	10.69050	10.91990	156	9.52	.595	.067	.053	7.440
13	10.76120	11.03500	159	9.63	.602	.069	.054	7.826
14	10.70600	10.96610	169	9.92	.620	.075	.059	8.680
15	10.78500	11.07960	164	9.76	.610	.071	.056	9.150
16	10.78155	11.06940	161	9.68	.605	.070	.055	9.680
17	10.79050	11.08140	160	9.64	.603	.069	.054	10.251

TABLE 7 - EXPERIMENTAL DATA FOR THE SAMPLES FIRED AT 900°C

Time (hr.)	Weight of the tube +Nickel Ferrite + Field off (gms.)	Weight of the tube +Nickel Ferrite + Field on. (gms.)	Susceptibility 10^{-6} (cgsm)	Bohr Magneton	Fraction of Ferrite formed (x)	$(x-(x-x^2))$	$1-x^2-(1-x)$	x^2
1	10.71320	10.87380	103	7.76	.685	.039	.031	.685
2	10.72780	10.95040	139	8.99	.562	.057	.045	1.124
3	10.72895	10.98750	161	9.68	.605	.070	.055	1.815
4	10.73000	11.03660	180	10.20	.640	.082	.064	2.560
5	10.71700	11.01320	189	10.49	.656	.080	.068	3.280
6	10.72130	11.03780	201	10.80	.676	.096	.076	4.056
7	10.72250	11.04170	201	10.80	.675	.096	.076	4.725
8	10.73170	11.06510	207	10.96	.685	.100	.077	5.480
9	10.72000	11.07910	228	11.52	.720	.118	.088	6.480
10	10.71645	11.05710	218	11.26	.704	.109	.083	7.040
11	10.72580	11.07200	222	11.36	.710	.112	.085	7.810
12	10.72370	11.06690	216	11.21	.701	.106	.082	8.412
13	10.71945	11.07830	227	11.45	.718	.113	.088	9.334
14	10.73630	11.08790	216	11.20	.700	.100	.082	9.800
15	10.72025	11.07070	223	11.37	.711	.113	.085	10.665
16	10.71620	11.05570	218	11.24	.703	.109	.083	11.248
17	10.71300	11.05200	220	11.20	.706	.110	.084	12.002

TABLE 8 - EXPERIMENTAL DATA FOR THE SAMPLES FIRED AT 930°C

Time (hr.)	Weight of the tube +Nickel Ferrite + Field off (grms)	Weight of the tube +Nickel Ferrite + Field on. (grms)	Susceptibility 10^{-6} (cgsm)	Bohr Magneton	Fraction of Ferrite formed (x)	$(1-(1-x)^{\frac{1}{3}})^2$	$1-\frac{2}{3}x-(1-x)^{\frac{2}{3}}$	χ_c
1	10.73475	10.94020	127	8.57	.536	.050	.040	.536
2	10.66025	10.88420	164	9.76	.610	.071	.056	1.220
3	10.70625	10.98930	186	10.38	.649	.085	.066	1.947
4	10.74865	10.09020	204	10.89	.681	.099	.076	2.724
5	10.70200	11.02990	217	10.23	.702	.108	.082	3.510
6	10.71475	11.06480	225	11.44	.715	.115	.087	4.290
7	10.76850	11.16590	228	11.52	.720	.118	.088	5.040
8	10.74640	11.16970	254	12.16	.760	.141	.103	6.080
9	10.79550	11.23540	240	11.80	.738	.128	.095	6.642
10	10.76200	11.18770	248	12.00	.750	.135	.099	7.500
11	10.76000	11.18170	246	11.96	.748	.134	.099	8.228
12	10.73535	11.14360	251	12.08	.755	.138	.101	9.060
13	10.81000	11.27680	248	12.00	.750	.135	.099	9.750
14	10.69890	11.08580	258	12.24	.765	.144	.105	10.710
15	10.76800	11.18740	242	11.84	.740	.129	.096	11.100
16	10.70300	11.09030	256	12.19	.762	.142	.104	12.182
17	10.74600	11.16680	253	12.13	.758	.140	.103	12.900

TABLE 9 - EXPERIMENTAL DATA FOR THE SAMPLES FIRED AT 1000°C

Time (hr.)	Weight of the tube +Nickel Ferrite + Field off (grms)	Weight of the tube +Nickel Ferrite + Field on. (grms)	Susceptibility 10^{-6} (cgsm)	Bohr Magneton	Fraction of Ferrite formed (x)	$(1-(1-x)^{1/3})^2$	$1-\frac{2}{3}x-(1-x)^{2/3}$	x^2
1	10.64640	10.89030	185	10.37	.648	.085	.066	.648
2	10.74210	11.13990	242	11.84	.740	.129	.096	1.480
3	10.73800	11.17730	269	12.49	.781	.155	.112	2.343
4	10.72575	11.20320	300	13.20	.825	.191	.133	3.300
5	10.75770	11.27820	306	13.33	.833	.199	.138	4.165
6	10.78255	11.33860	311	13.44	.840	.206	.142	5.040
7	10.79265	11.37450	320	13.61	.851	.218	.148	5.957
8	10.76450	11.31400	319	13.60	.850	.217	.147	6.800
9	10.74310	11.27900	325	13.73	.858	.226	.152	7.722
10	10.76025	11.30760	320	13.63	.852	.219	.149	8.520
11	10.74980	11.29570	326	13.76	.860	.228	.153	9.460
12	10.79360	11.39160	328	13.79	.862	.230	.155	10.344
13	10.79900	11.41300	333	13.90	.869	.239	.159	11.307
14	10.78350	11.37620	330	13.84	.865	.234	.157	12.110
15	10.91105	11.65040	332	13.87	.867	.236	.158	13.005
16	10.91235	11.64130	326	13.76	.860	.228	.153	13.760
17	10.96320	11.76410	332	13.89	.868	.238	.159	14.800

TABLE 10 - EXPERIMENTAL DATA FOR THE SAMPLES FIRED AT 1100°C

Time (hr.)	Weight of the tube +Nickel Ferrite + Field off (grms)	Weight of the tube +Nickel Ferrite + Field on. (grms)	Susceptibility 10^{-6} (cgsm)	Bohr Magneton	Fraction of Ferrite formed (x)	$(1-(1-x)^{1/3})^2$	$1-\frac{2x}{3}-(1-x)^{2/3}$	Kt
1	10.85200	11.41260	277	12.67	.792	.164	.117	.792
2	10.82130	11.43900	322	13.66	.854	.221	.150	1.708
3	10.81860	11.48620	349	14.24	.890	.268	.174	2.670
4	10.88340	11.66310	365	14.56	.910	.301	.189	3.640
5	10.91200	11.75480	377	14.80	.925	.330	.202	4.625
6	10.93750	11.82490	382	14.89	.931	.344	.208	5.586
7	10.93850	11.83490	386	14.96	.935	.355	.212	6.545
8	10.96230	11.89040	386	14.96	.935	.355	.212	7.480
9	10.93805	11.84350	390	15.04	.940	.366	.217	8.460
10	10.89850	11.75980	394	15.13	.945	.379	.223	9.450
11	10.93750	11.82300	382	14.88	.930	.341	.207	10.230
12	10.96300	11.91400	395	15.13	.946	.382	.224	11.352
13	10.96206	11.94210	407	15.37	.961	.432	.242	12.493
14	10.84995	11.64360	393	15.10	.944	.377	.221	13.216
15	10.95030	11.89900	398	15.20	.950	.394	.228	14.250
16	10.98200	11.97130	400	15.23	.952	.401	.231	15.232
17	10.97850	11.94860	398	15.20	.949	.394	.228	16.500

TABLE 11 - K VALUES CALCULATED FOR JANDER REACTION MODEL

S.N.	K	Log K	T (^{o}K)	$\frac{1}{T} \times 10^{4}$
1	0.0004	-3.3979	973	10.30
2	0.0022	-2.6576	1073	9.32
3	0.0050	-2.3010	1123	8.90
4	0.0100	-2.0000	1148	8.72
5	0.0140	-1.8539	1173	8.52
6	0.0168	-1.7747	1203	8.30
7	0.0340	-1.4685	1273	7.85
8	0.0520	-1.2840	1373	7.28

TABLE 12 - K VALUES CALCULATED FOR GINSTLING - BROUNSHTEIN MODEL

S.N.	K	Log K	T(^{o}K)	$\frac{1}{T} \times 10^{4}$
1	0.0002	-3.6990	973	10.30
2	0.0023	-2.6289	1073	9.32
3	0.0039	-2.4089	1123	8.90
4	0.0100	-2.0000	1148	8.71
5	0.0110	-1.9586	1173	8.52
6	0.0125	-1.9031	1203	8.30
7	0.0230	-1.6383	1273	7.85
8	0.0290	-1.5376	1373	7.28

TABLE 13 - K VALUES CALCULATED FOR MODIFIED GINSTLING - BROUNSHTEIN MODEL

S.N.	K	Log K	T(^{o}K)	$\frac{1}{T} \times 10^{4}$
1	0.0262	-1.5819	973	10.30
2	0.1051	-0.9784	1073	9.32
3	0.1763	-0.7537	1123	8.90
4	0.3443	-0.4630	1148	8.72
5	0.5206	-0.2835	1173	8.52
6	0.5774	-0.2386	1203	8.30
7	0.9657	-0.0152	1273	7.85
8	1.2131	+0.0839	1373	7.28

TABLE 14 - K VALUES CALCULATED FOR KROGER - ZIEGLER REACTION MODEL

S.N.	K	Log K	T(^{o}K)	$\frac{1}{T} \times 10^{4}$
1	0.0262	-1.5819	873	10.30
2	0.0612	-1.2135	1073	9.32
3	0.1051	-0.9784	1123	8.90
4	0.2126	-0.6725	1148	8.72
5	0.3541	-0.4509	1173	8.52
6	0.4142	-0.3827	1203	8.30
7	0.7813	-0.1072	1273	7.85
8	1.1504	+0.0608	1373	7.28

TABLE 15 - FRACTION OF FERRITE FORMED OBTAINED BY MAGNETIC AND CHEMICAL ANALYSIS METHODS

S.N.	Temperature (^{o}C)	Time (hr.)	Fraction of ferrite formed(x)	
			Magnetic measurement	Chemical Analysis
1	2	3	4	5
1	700	1	.235	.253
2	700	5	.281	.290
3	700	9	.286	.293
4	700	14	.300	.309
5	800	6	.375	.376
6	800	10	.393	.396
7	800	13	.388	.389
8	800	16	.396	.398
9	850	2	.380	.384
10	850	7	.460	.461
11	850	11	.479	.471
12	850	17	.450	.453
13	875	3	.516	.514
14	875	8	.582	.580
15	875	13	.602	.605
16	875	17	.603	.601
17	900	1	.485	.480
18	900	8	.685	.682

Contd....

1	2	3	4	5
19	900	12	.701	.700
20	900	16	.703	.698
21	930	4	.681	.679
22	930	8	.760	.757
23	930	13	.750	.750
24	930	17	.758	.755
25	1000	1	.648	.644
26	1000	6	.840	.838
27	1000	10	.852	.853
28	1000	17	.868	.864
29	1100	3	.890	.890
30	1100	9	.940	.937
31	1100	14	.944	.943
32	1100	17	.949	.947

Table 16 - Activation energies Calculated by Different Reaction Models.

S.N.	Model	Activation energy (Kcal/mole)
1.	Jander	47.55
2.	Ginstling-Brounshtein	46.26
3.	Modified Ginstling-Brounshtein	31.28
4.	Kroger - Ziegler	30.82

Table 17 - Ionic Radii of Elements

S.N.	Ions	Ionic Radii according to Goldschmidt[58].
1.	O^{2-}	1.32
2	Mg^{2+}	0.78
3	Al^{3+}	0.57
4	Mn^{2+}	0.91
5	Mn^{3+}	0.70
6	Fe^{3+}	0.67
7	Fe^{2+}	0.83
8	Co^{2+}	0.82
9	Ni^{2+}	0.78
10	Zn^{2+}	0.83

$$\mu_{eff} = 2.84 \sqrt{SM \times T}$$

where T is the temperature in kelvin at which the observations are taken. In our case

$$T = 273 + 32 = 305$$

The unit of μ_{eff} is Bohr magneton. The total number of Bohr magneton in pure nickel ferrite is 16. So the fraction of ferrite formed may be calculated by dividing the μ_{eff} with 16.

$$X = \frac{\mu_{eff}}{16}$$

APPENDIX B

CALCULATION OF TUBE CONSTANT

The calibration of tube was done by ferric oxide of known susceptibility and also confirmed with nickel oxide. The procedure of tube constant calculation is given below

Weight of the empty tube + Field off = 10.26480

Weight of the empty tube + Field on = 10.26480

Weight of the empty tube + Ferric oxide = 10.78520

Weight of the empty tube + Ferric oxide + Field on = 10.72214

$W = 10.78520 - 10.26480 = 0.52040$

$W = (10.72214 - 10.78520) \times 1000$

$= 36.940$

$S_{Fe_2O_3} = 20.6 \times 10^{-6}$

$$C = \frac{20.6 \times 10^{-6} \times .52040}{36.940}$$

$= 0.29 \times 10^{-6}$

CALCULATION OF FRACTION OF FERRITE FORMED

Susceptibility S $= C\frac{\Delta W}{W}$

Molar susceptibility $= SM = S \times$ Mol.wt.

$= S \times 235$

$$\mu eff = 2.84 \sqrt{SM \times T}$$

where T is the temperature in kelvin at which the observations are taken. In our case

$$T = 273 + 32 = 305$$

The unit of μeff is Bohr magneton. The total number of Bohr magneton in pure nickel ferrite is 16. So the fraction of ferrite formed may be calculated by dividing the μeff with 16.

$$X = \frac{\mu eff}{16}$$